Electronic Supplementary Material (ESI) for ChemComm.

Supporting Information

Unusual selectivity in the ring-opening of γ-valerolactone oxide by amines

Zahra Mazloomi,[a] Fabian Kallmeier,[a] Sarah Kirchhecker,[a] Bernhard Stadler,[a] Swechchha Pandey,[a] Claas Schünemann,[a] Anke Spannenberg,[a] Christian Hering-Junghans,[a] Sergey Tin,[a] Johannes G. de Vries,[a,*] Eszter Baráth[a,*]

[a]Leibniz Institut für Katalyse e.V. (LIKAT) Albert Einstein Str.29a, D-18059 Rostock (Germany)
*E-mail: Johannes.deVries@catalysis.de, Eszter.Barath@catalysis.de

Table of content

Chemicals
Propylamine (99%), *tert*-butylamine (98%), dibenzylamine (99%) and α-angelica lactone (98%), anhydrous acetonitrile (99.8%) were purchased from Sigma Aldrich. Hexylamine (99%), isopropylamine (99%), benzylamine (99%), cyclohexylamine (99%) and diethylamine were purchased from TCI. Octylamine (99%), tetrahydrofuran, dichloromethane, toluene and dimethylformamide were purchased from Acros Organics.

Methods
^{1}H-NMR / ^{13}C-NMR Spectra were recorded at room temperature on 300 MHz spectrometers (Avance 300 or Fourier 300) or a 400 MHz spectrometer (Avance 400) from Bruker. The chemical shifts (δ) are given in ppm and referenced to the residual proton signal of the corresponding solvent.

GC Measurements were carried out on an Agilent 7890B-GC-System equipped with a 30 m x 320 µm x 0.25 µm poly-methylsiloxane column and a flame ionization detector.

ESI Mass spectrometry was recorded on an Agilent 1260/6130 Quadrupol LC-MS equipped with a time-of-flight detector.

For the quantification of **CHN**, a microanalyzer-TruSpec CHNS (Leco) was used. The samples were catalytically combusted with pure oxygen in a helium stream. For the analysis of C and H contents an IR-detector was used.

ATR-IR measurements were recorded on a Nicolet iS5 FT-IR (Thermo Fisher) device, calibrated on 1.5 mil polystyrene, and equipped with a GladiATR 210 accessory from PIKE technologies.

Solvent screening
Table S1. Solvent screening using 1 equiv. of hexylamine to GVLO.

Entry	Reaction time	Solvent	Conversion (%)[a]
1	5 min	-	>99
2	20 min	Toluene	80
3	60 min	Toluene	98
4	20 min	DCM	80
5	60 min	DCM	95
6	20 min	MeCN	80
7	60 min	MeCN	95
8	20 min	DMF	30
9	60 min	DMF	70

[a]Conversion was determined by ^{1}H NMR.

Experimental procedures

Preparation of β-angelica lactone (β-AL)[1]

α-Angelica lactone (98%, 120g, 1.2 mol) was added to a 250 mL two neck flask equipped with a condenser and a magnetic stirrer followed by the addition of triethylamine (5 mol%, 8.5 mL). The mixture was heated to 100°C under an argon atmosphere. After 1.5 hours a ratio of β/α-angelica lactone of 90-95/10-5 was reached, the reaction allowed to cool down to room temperature and the condenser exchanged with a distillation head. Subsequent vacuum distillation at 6×10^{-2} mbar yielded two fractions: 38-42°C containing mainly the α-isomer. 45-50°C yielded a mixture of angelica lactones with 90 mol% content of the β-isomer (106 g, 88%). **Note:** Ideally the whole procedure should be conducted in one day, as prolonged exposure of the angelica lactone mixture to triethylamine results in an increased formation of dimers and oligomers.

This mixture was then further purified by a second distillation. A first fraction at (T(bath)=53°C; T(head)= 35-36°C, p= $1.6\ 10^{-1}$ mbar) was collected that consisted almost entirely of α-angelica lactone. **Note:** It is recommended to analyze the bottom regularly to ensure complete removal of the α-AL). After removal of this fraction, β-AL could be collected ((T(bath)= 65°C; T(head)= 40°C, p= $2.2\ 10^{-1}$ mbar). (After the second distillation, isolated yield: 38%; purity >98% (GC).)

^{1}H NMR (400 MHz, CD_2Cl_2) δ 7.46 (dd, $^3J_{H\text{-}H}$ = 5.7, 1.5 Hz, 1H), 6.04 (dd, $^3J_{H\text{-}H}$ = 5.7, 2.0 Hz, 1H), 5.11 (qt, $^3J_{H\text{-}H}$ = 6.9, 2.0, 1.5 Hz, 1H), 1.41 (d, J = 6.9 Hz, 3H). **^{13}C NMR** (101 MHz, CD_2Cl_2) δ 173.3, 158.0, 121.3, 80.0, 19.0.

Synthesis of the γ-valerolactone oxide (GVLO)

In a 5 L glass reactor (with efficient cooling and overhead stirrer) was placed 1 L MeCN and β-angelica lactone (98.1 g, 1 mol) and the mixture was subsequently cooled to 0 °C using a cryostat. Then, NaOCl x $5H_2O$ (411.3 g, 2.5 mol, 2.5 eq.) was added in small portions under vigorous stirring, so that a temperature below 5 °C was strictly maintained. [**Note 1**] After the addition was completed, the reaction progress was monitored *via* GC. Typically, after 6 hours (from the initial sodium hypochlorite addition) the reaction reached a maximum conversion. [**Note 2**] At this point, small amounts of Na_2SO_3 were added until the yellow-green color of the reaction mixture disappeared [**Note 3**], again ensuring that the temperature does not exceed 5 °C. The reaction was allowed to warm to room temperature and the solids were filtered off. The solution was evaporated under reduced pressure, and the resulting yellow oil was diluted with 0.5 L diethyl ether. Copious amounts of dissolved sodium chloride precipitated out of solution and 0.25 L *n*-pentane was added to fully precipitate the salt. Afterwards, the solid was filtered off and the clear solution placed into a freezer (-80 °C). The colorless crystals of GVLO were filtered off and recrystallized from 0.35 L diethyl ether at -80 °C to furnish 30 to 35 g GVLO (26 - 31 %) [**Note 4**] in sufficient purity (> 98 % by GC).

^{1}H NMR (300 MHz, C_6D_6): δ = 4.02 (qd, $^3J_{H\text{-}H}$ = 6.7, 0.8 Hz, 1H), 3.22 (dd, $^3J_{H\text{-}H}$ = 2.6, 0.8 Hz, 1H), 2.99 (d, $^3J_{H\text{-}H}$ = 2.6 Hz, 1H), 0.67 (d, $^3J_{H\text{-}H}$ = 6.7 Hz, 3H) ppm; **^{13}C NMR** (75 MHz, C_6D_6): δ = 170.3, 75.9, 58.6, 49.8, 17.1 ppm. For complete characterization of GVLO please see ref 2.[2]

[Note 1]: If the temperature rises to about 15 °C, an exothermic runaway reaction takes place. The temperature only spikes after a slight delay after adding NaOCl. During the runaway reaction, the solvent starts to boil, and it is nearly impossible to filter the obtained mixture afterwards, probably due to large amounts of polymer being formed, significantly lowering the overall yield.

[Note 2]: The ratio between GVLO and starting material at this point will be 90 / 10.

[Note 3]: The exact amount of Na_2SO_3 required for the complete quench varied from run to run but was typically around 15 g sodium sulfite per mol of SM.

[Note 4]: The epoxide from the supernatant could be partially recovered by Dry Column Vacuum Chromatography (DCVC, 25 cm, Ø 7 cm, 500 mL per fraction), using toluene (3 parts by volume) and *tert*-butyl methyl ether (1 parts by volume) as eluent. Typically, the supernatant of multiple reactions was combined, so an exact yield cannot be given. It was however noted, that in small test runs near quantitative recovery was possible. It was observed that epoxide decomposed on silica at higher temperature (approx. 40 °C) during column chromatography.

Synthesis of oxirane-carboxamides (2) and dihydroxyamides (3)

Note: Strictly for preparative reason, to determine the corresponding isolated yields of the given products, in some cases we used different substrate/amine ratio (than 1:1 or 1:2) and different reaction times as it is given in the discussion part of the manuscript. Please see below the exact preparation routes for product series **2** and **3**.

3-(1-hydroxyethyl)-N-propyloxirane-2-carboxamide (2a)
γ-Valerolactone oxide (57 mg, 0.50 mmol) was reacted with n-propylamine (41 µL, 0.50 mmol) in neat at RT for 1 h. The mixture was dissolved in DCM and the solution was extracted 2 x with water and once with brine. The aqueous part was extracted once with DCM. The organic layer was separated, combined and dried over anhydrous $MgSO_4$. The solvent was evaporated, and the product was obtained as white solid (84 mg, 97%).
^{1}H NMR (300 MHz, $CDCl_3$) δ : 6.24 (s, 1H), 3.57 (d, $^3J_{H-H}$ = 4.6 Hz, 1H), 3.49 (dq, $^3J_{H-H}$ = 8.1, 6.3 Hz, 1H), 3.30 – 3.20 (m, 2H), 3.07 (dd, $^3J_{H-H}$ = 8.2, 4.6 Hz, 1H), 2.99 (s, 1H), 1.54 (h, $^3J_{H-H}$ = 7.2 Hz, 2H), 1.36 (d, $^3J_{H-H}$ = 6.3 Hz, 3H), 0.93 (t, $^3J_{H-H}$ = 7.4 Hz, 3H). **^{13}C NMR** (75 MHz, $CDCl_3$) δ : 167.3, 77.1, 65.3, 61.0, 55.4, 40.9, 22.8, 20.4, 11.4. **HR MS (ESI+)**: m/z calculated for $[M + H]^+$: 174.1130, found: 174.1131. **IR**: ν (OH, HN-C=O) = 3262 cm^{-1}, ν (C=O) = 1639 cm^{-1}, ν (-C-O-C-) = 937 cm^{-1}.

3-(1-hydroxyethyl)-N-isopropyloxirane-2-carboxamide (2b)
γ-Valerolactone oxide (57 mg, 0.50 mmol) was reacted with isopropylamine (43 µL, 0.50 mmol) in neat at RT for 1 h. The mixture was dissolved in DCM and the solution was extracted 2 x with water and once with brine. The aqueous part was extracted once with DCM. The organic layer was separated, combined and dried over anhydrous $MgSO_4$. The solvent was evaporated, and the product was obtained as colorless liquid (82 mg, 95%).
^{1}H NMR (300 MHz, $CDCl_3$) δ : 6.02 (s, 1H), 4.11 (dp, $^3J_{H-H}$ = 8.3, 6.6 Hz, 1H), 3.54 (d, $^3J_{H-H}$ = 4.6 Hz, 1H), 3.52 – 3.44 (m, 1H), 3.07 (dd, $^3J_{H-H}$ = 8.1, 4.6 Hz, 1H), 1.37 (d, $^3J_{H-H}$ = 6.3 Hz, 3H), 1.17 (dd, $^3J_{H-H}$ = 8.6, 6.6 Hz, 6H). **^{13}C NMR** (75 MHz, $CDCl_3$) δ : 166.4, 77.1, 65.4, 61.0, 55.2, 41.4, 22.8, 22.6, 20.4. **HR MS (ESI+)**: m/z calculated for $[M + H]^+$: 174.1130, found: 174.1134. **IR**: ν (OH, HN-C=O) = 3242 cm^{-1}, ν (C=O) = 1642 cm^{-1}, ν (-C-O-C-) = 927 cm^{-1}.

N-(tert-butyl)-3-(1-hydroxyethyl)oxirane-2-carboxamide (2c)
γ-Valerolactone oxide (57 mg, 0.50 mmol) was reacted with tert-butylamine (78 µL, 0.75 mmol) in neat at RT for 6 h. The mixture was dissolved in DCM and the solution was extracted 2 x with water and once with brine. The aqueous part was extracted once with DCM. The organic layer was separated, combined and dried over anhydrous $MgSO_4$. The solvent was evaporated, and the product was obtained as white solid (90 mg, 97%).
^{1}H NMR (300 MHz, $CDCl_3$) δ: 6.01 (s, 1H), 3.51 (dt, $^3J_{H-H}$ = 8.2, 6.3 Hz, 1H), 3.46 (d, $^3J_{H-H}$ = 4.6 Hz, 1H), 3.03 (dd, $^3J_{H-H}$ = 8.2, 4.6 Hz, 1H), 1.35 (d, $^3J_{H-H}$ = 6.3 Hz, 12H). **^{13}C NMR** (75 MHz, $CDCl_3$) δ: 166.6, 77.1, 65.3, 61.1, 55.4, 51.8, 28.7, 20.4. **HR MS (ESI+)**: m/z calculated for $[M + H]^+$: 210.1105, found: 210.1106. **IR**: ν (OH, HN-C=O) = 3284 cm^{-1}, ν (C=O) = 1647 cm^{-1}, ν (-C-O-C-) = 911 cm^{-1}.

N-hexyl-3-(1-hydroxyethyl)oxirane-2-carboxamide (2d)
γ-Valerolactone oxide (57 mg, 0.50 mmol) was reacted with hexylamine (66 µL, 0.50 mmol) in neat at RT for 5 min. The product was obtained as white solid (107 mg, quantitative).
^{1}H NMR (300 MHz, $CDCl_3$) δ: 6.21 (s, 1H), 3.56 (d, $^3J_{H-H}$ = 4.6 Hz, 1H), 3.54 – 3.42 (m, 1H), 3.33 – 3.21 (m, 2H), 3.07 (dd, $^3J_{H-H}$ = 8.2, 4.6 Hz, 1H), 2.93 (s, 1H), 1.49 (dd, $^3J_{H-H}$ = 14.3, 6.7 Hz, 2H), 1.36 (d, $^3J_{H-H}$ = 6.3 Hz, 3H), 1.33 – 1.19 (m, 6H), 0.94 – 0.83 (m, 3H). **^{13}C NMR** (75 MHz, $CDCl_3$) δ: 167.3, 77.1, 64.6, 61.1, 55.4, 39.1, 31.4, 29.3, 26.5, 22.5, 20.4, 14.0. **HR MS (ESI+)**: m/z calculated for $[M + H]^+$: 216.1599, found: 216.1600. **IR**: ν (OH, HN-C=O) = 3293 cm^{-1}, ν (C=O) = 1637 cm^{-1}, ν (-C-O-C-) = 909 cm^{-1}.

N-benzyl-3-(1-hydroxyethyl)oxirane-2-carboxamide (2e)

γ-Valerolactone oxide (57 mg, 0.50 mmol) was reacted with benzylamine (60 µL, 0.55 mmol) in neat at RT for 15 min. The mixture was dissolved in DCM and the solution was extracted 2 x with water and once with brine. The aqueous part was extracted once with DCM. The organic layer was separated, combined and dried over anhydrous $MgSO_4$. The solvent was evaporated, and the product was obtained as white solid (108 mg, 98%).

^{1}H NMR (400 MHz, $CDCl_3$) δ: 7.34 – 7.13 (m, 5H), 6.56 (s, 1H), 4.48 – 4.26 (m, 2H), 3.51 (d, $^3J_{H-H}$ = 4.5 Hz, 1H), 3.44 (dq, $^3J_{H-H}$ = 8.1, 6.3 Hz, 1H), 3.32 (s, 1H), 2.99 (dd, $^3J_{H-H}$ = 8.1, 4.6 Hz, 1H), 1.25 (d, $^3J_{H-H}$ = 6.4 Hz, 3H). **^{13}C NMR** (101 MHz, $CDCl_3$) δ: 167.3, 137.3, 128.9, 127.9, 127.9, 77.1, 65.0, 61.2, 55.3, 43.2, 20.4. **HR MS (ESI+)**: m/z calculated for $[M + H]^+$: 214.1443, found: 214.1440. **Anal. Calcd. for** $C_{12}H_{15}NO_3$: C, 65.14; H, 6.83; N, 6.33. Found: C, 65.42; H, 7.41; N, 5.82. **IR:** ν (OH, HN-C=O) = 3328 cm^{-1}, ν (C=O) = 1630 cm^{-1}, ν (-C-O-C-) = 915 cm^{-1}.

N-cyclohexyl-3-(1-hydroxyethyl)oxirane-2-carboxamide (2f)

γ-Valerolactone oxide (57 mg, 0.50 mmol), 50 µL of MeCN was added and it was reacted with cyclohexylamine (57 µL, 0.50 mmol) at RT for 15 min. The solvent was removed under reduced pressure and the product was obtained as white solid (106 mg, quantitative).

^{1}H NMR (300 MHz, $CDCl_3$) δ: 6.12 (d, *J* = 8.8 Hz, 1H), 3.84 – 3.69 (m, 1H), 3.65 – 3.23 (m, 3H), 3.05 (dd, $^3J_{H-H}$ = 8.2, 4.6 Hz, 1H), 1.95 – 1.81 (m, 2H), 1.76 – 1.55 (m, 3H), 1.34 (d, $^3J_{H-H}$ = 6.3 Hz, 5H), 1.23 – 1.05 (m, 3H). **^{13}C NMR** (75 MHz, $CDCl_3$) δ: 166.3, 77.1, 64.9, 61.1, 55.3, 48.1, 33.1, 32.8, 25.4, 24.8, 20.4. **HR MS (ESI+)**: m/z calculated for $[M + H]^+$: 214.1443, found: 214.1440. **IR**: ν (OH, HN-C=O) = 3293 cm^{-1}, ν (C=O) = 1637 cm^{-1}, ν (-C-O-C-) = 908 cm^{-1}.

3-(1-hydroxyethyl)-N-octyloxirane-2-carboxamide (2g)

γ-Valerolactone oxide (57 mg, 0.50 mmol) was reacted with octylamine (91 µL, 0.55 mmol) in neat at RT for 30 min. The mixture was dissolved in DCM and the solution was extracted 2 x with water and once with brine. The aqueous part was extracted once with DCM. The organic layer was separated, combined and dried over anhydrous $MgSO_4$. The solvent was evaporated, and the product was obtained as white solid (119 mg, 98%).

^{1}H NMR (300 MHz, $CDCl_3$) δ : 6.20 (s, 1H), 3.50 (d, $^3J_{H-H}$ = 4.6 Hz, 1H), 3.48 – 3.38 (m, 1H), 3.30 (s, 1H), 3.24 – 3.16 (m, 2H), 3.01 (dd, $^3J_{H-H}$ = 8.2, 4.6 Hz, 1H), 1.50 – 1.40 (m, 2H), 1.30 (d, $^3J_{H-H}$ = 6.3 Hz, 2H), 1.22 (d, $^3J_{H-H}$ = 4.0 Hz, 12H), 0.84 – 0.78 (m, 3H). **^{13}C NMR** (75 MHz, $CDCl_3$) δ: 167.2, 77.1, 65.1, 61.1, 55.4, 39.2, 31.8, 29.5, 29.2, 26.9, 22.7, 20.4, 14.1. **HR MS (ESI+)**: m/z calculated for $[M + H]^+$: 244.1912, found: 244.1918. **Anal. Calcd for** $C_{13}H_{25}NO_3$: C, 64.16; H, 10.36; N, 5.76. Found: C, 64.14; H, 10.33; N, 5.47. **IR**: ν (OH, HN-C=O) = 3294 cm^{-1}, ν (C=O) = 1652 cm^{-1}, ν (-C-O-C-) = 894 cm^{-1}.

N,N-diethyl-3-(1-hydroxyethyl)oxirane-2-carboxamide (2h)

γ-Valerolactone oxide (57 mg, 0.50 mmol) was reacted with diethylamine (62 µL, 0.60 mmol) in neat at RT for 4 h. The mixture was dissolved in DCM and the solution was extracted 2 x with water and once with brine. The aqueous part was extracted once with DCM. The organic layer was separated, combined and dried over anhydrous $MgSO_4$. The solvent was evaporated, and the product was obtained as pale yellow solid (90 mg, 97%).

^{1}H NMR (400 MHz, $CDCl_3$) δ : ^{1}H NMR (300 MHz, $CDCl_3$) δ 3.90 (s, 1H), 3.62 – 3.46 (m, 3H), 3.45 – 3.29 (m, 3H), 3.03 (dd, $^3J_{H-H}$ = 8.1, 4.3 Hz, 1H), 1.36 (d, $^3J_{H-H}$ = 6.2 Hz, 3H), 1.24 (t, $^3J_{H-H}$ = 7.2 Hz, 3H), 1.14 (t, $^3J_{H-H}$ = 7.2 Hz, 3H). **^{13}C NMR** (75 MHz, $CDCl_3$) δ: 166.7, 77.1, 68.0, 60.4, 54.5, 42.0, 40.1, 20.1, 14.4, 12.7. **HR MS (ESI+)**: m/z calculated for $[M + H]^+$: 188.1286, found: 188.1283. **Anal. Calcd. for** $C_9H_{17}NO_3$: C, 57.73; H, 9.15; N, 7.48. Found: C, 57.51; H, 9.04; N, 7.08. **IR**: ν (OH, -N-C=O) = 3358 cm^{-1}, ν (C=O) = 1627 cm^{-1}, ν (-C-O-C-) = 900 cm^{-1}.

***N*-isopropyl-3-(isopropylamino)-2,4-dihydroxypentanamide (3b)**

γ-Valerolactone oxide (114 mg, 1.0 mmol) was reacted with isopropylamine (171 µL, 2.0 mmol) in neat at RT for 1 h. The product was obtained as white solid (231 mg, quantitative).

^{1}H NMR (300 MHz, $CDCl_3$) δ : 6.11 (s, 1H), 4.13 – 3.95 (m, 1H), 3.50 – 3.37 (m, 2H), 3.09 – 2.95 (m, 2H), 2.86 (s, 1H), 1.29 (d, $^3J_{H-H}$ = 6.3 Hz, 3H) , 1.11 (dd, $^3J_{H-H}$ = 8.4 Hz, $^3J_{H-H}$ = 6.6 Hz, 7H) , 1.01 (d, $^3J_{H-H}$ = 6.2 Hz, 5H). **^{13}C NMR** (75 MHz, $CDCl_3$) δ: 166.3, 63.9, 61.4, 55.3, 42.6, 41.2, 25.7, 22.7, 22.4, 20.5. **HR MS (ESI+)**: m/z calculated for $[M + H]^+$: 233.1860, found: 233.1861. **IR**: ν (OH, NH, HN-C=O) = 3241 cm^{-1}, ν (C=O) = 1648 cm^{-1}.

***N*-hexyl-3-(hexylamino)-2,4-dihydroxypentanamide (3d)**

γ-Valerolactone oxide (57 mg, 0.5 mmol) was reacted with hexylamine (131 µL, 1.0 mmol) in neat at RT for 1 h. The product was obtained as colorless dense liquid (158 mg, quantitative).

^{1}H NMR (300 MHz, $CDCl_3$) δ : 6.22 (s, 1H), 3.55 (d, $^3J_{H-H}$ = 4.6 Hz, 1H), 3.51 – 3.42 (m, 1H), 3.31 – 3.23 (m, 2H), 3.06 (dd, $^3J_{H-H}$ = 8.3, 4.6 Hz, 1H), 2.69 – 2.60 (m, 2H), 2.17 (s, 2H), 1.58 – 1.37 (m, 4H), 1.35 (d, $^3J_{H-H}$ = 6.3 Hz, 3H), 1.33 – 1.19 (m, 12H), 0.92 – 0.81 (m, 6H). **^{13}C NMR** (75 MHz, $CDCl_3$) δ: 167.2, 77.1, 64.0, 61.3, 55.5, 41.9, 39.0, 33.4, 31.6, 31.3, 29.3, 26.5, 22.6, 22.5, 20.4, 14.0, 13.9. **HR MS (ESI+)**: m/z calculated for $[M + H]^+$: 317.2804, found: 317.2798. **IR**: ν (OH, NH, HN-C=O) = 3334 cm^{-1}, ν (C=O) = 1649 cm^{-1}.

***N*-cyclohexyl-3-(cyclohexylamino)-2,4-dihydroxypentanamide (3f)**

γ-Valerolactone oxide (114 mg, 1.0 mmol) was reacted with cyclohexylamine (229 µL, 2.0 mmol) in neat at RT for 1 h. The product was obtained as white solid (311 mg, quantitative).

^{1}H NMR (300 MHz, $CDCl_3$) δ: 6.14 (d, $^3J_{H-H}$ = 8.7 Hz, 1H), 3.77 – 3.62 (m, 1H), 3.46 – 3.33 (m, 2H), 3.14 – 2.74 (m, 3H), 2.51 (qt, $^3J_{H-H}$ = 10.5 Hz, $^3J_{H-H}$ = 3.9 Hz, 1H), 1.89 – 1.44 (m, 10H), 1.37 – 0.86 (m, 12H). **^{13}C NMR** (75 MHz, $CDCl_3$) δ: 166.2, 63.6, 61.5, 55.4, 50.2, 47.9, 36.4, 33.1, 32.7, 25.5, 25.3, 25.1, 24.7, 20.5. **HR MS (ESI+)**: m/z calculated for $[M + H]^+$: 313.2486, found: 313.2497. **IR**: ν (OH, NH, HN-C=O) = 3230 cm^{-1}, ν (C=O) = 1644 cm^{-1}.

***N*-octyl-3-(octylamino)-2,4-dihydroxypentanamide (3g)**

γ-Valerolactone oxide (114 mg, 1.0 mmol) was reacted with octylamine (331 µL, 2.0 mmol) in neat at RT for 1 h. The product was obtained as white solid (371 mg, quantitative).

^{1}H NMR (300 MHz, $CDCl_3$) δ : 6.30 (s, 1H), 3.50 (d, $^3J_{H-H}$ = 4.5 Hz, 1H), 3.46 – 3.38 (m, 1H), 3.22 (q, $^3J_{H-H}$ = 6.8 Hz, 2H), 3.02 (dd, $^3J_{H-H}$ = 8.1 Hz, $^3J_{H-H}$ = 4.6 Hz, 1H), 2.79 – 2.46 (m, 4H), 1.52 – 1.34 (m, 4H), 1.33 – 1.15 (m, 23H), 0.88 – 0.80 (m, 6H). **^{13}C NMR** (75 MHz, $CDCl_3$) δ: 167.2, 64.1, 61.4, 55.5, 42.0, 39.1, 33.5, 31.8, 31.7, 29.4, 29.3, 29.2, 26.9, 22.7, 22.6, 20.4, 14.1, 14.0. **HR MS (ESI+)**: m/z calculated for $[M + H]^+$: 373.3425, found: 373.3430. **IR**: ν (OH, NH, HN-C=O) = 3332 cm^{-1}, ν (C=O) = 1641 cm^{-1}.

Reactivity trend of amines

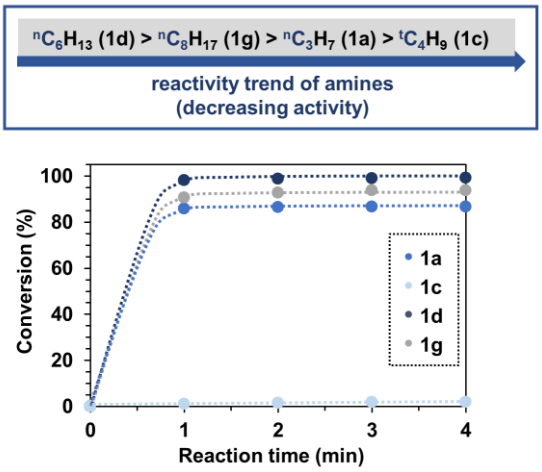

Figure S1. Reactivity trend of the tested amines (using 1eq.), showing the strict dependence on steric bulkiness.

Computational details

Computations were carried out using Gaussian16[3] the standalone version of NBO 6.0.[4,5]

Structure optimizations employed the B3LYP hybrid DFT functional[6] in conjunction with Grimme's dispersion correction D3(BJ)[7] and the def2-TZVP basis set[8] (notation B3LYP-D3/def2-TZVP). All structures were fully optimized and confirmed as minima (0 imaginary frequencies) by frequency analyses. Partial charges were determined by Natural Population analysis (NPA) using the NBO program. Fukui analyses were performed using MultiWfn 3.6[9] employing Gaussian16 formatted checkpoint files at the B3LYP-D3/6-31G(d) level of theory.

Summary of calculated data

Table S2. Summary of calculated data, including electronic energies and thermal corrections.

Compd.	NIMAG	ZPE (kcal·mol^{-1})	E_{tot}[a]	H_{298}[b]	G_{298}[c]
GVLO	0	67.3125	-419.9656	-419.8508	-419.8893

[a]Total SCF energy in a.u. [b]E_{tot} + thermal correction to enthalpy in a.u. (298 K unless stated otherwise). [c]E_{tot} + thermal correction to Gibbs free energy in a.u. (298 K unless stated otherwise).

Bonding, NBO analysis and Fukui analysis

GVLO

We first inspected the Kohn-Sham-orbitals of GVLO at the B3LYP-D3/def2-TZVP level of theory. This revealed the LUMO to show a large contribution (39%, according to Mulliken partition) on the lactone carbonyl atom, in line with the nucleophilic attack at this side. Figure S2 shows the most important KS-orbitals.

Figure S2. Relevant Kohn-Sham orbitals of GVLO (B3LYP-D3/def2-TZVP).

Next an NBO analysis was carried out on the B3LYP/aug-cc-pvtz//B3LYP-D3/def2-TZVP level of theory to determine nucleophilic sites by inspection of the natural charges. This clearly shows that the lactone carbonyl atom (C4) carries a considerable positive charge (+0.75 e), compared to the C-atoms of the epoxide unit (C2: 0.06; C3: -0.03 e) and is thus the favored center for nucleophilic attack. Moreover, the π*-interaction of the C=O unit in the lactone ring is strongly polarized towards C, making this the pronounced nucleophilic center in the molecule. The nucleophilicity can be further rationalized by the fact that all bonds around C4 are polarized towards the respective bonding partners (O5, O6, C3).

NPA-Charges

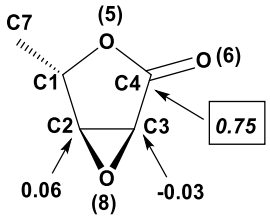

NPA Charges

C 1 0.09690

C 2 0.05744

C 3 -0.02798

C 4 0.75464

O 5 -0.51311

O 6 -0.53401

C 7 -0.60090

O 8 -0.48885

Bonding

20. (1.97390) BD (1) C 2- O 8
(34.71%) 0.5892* C 2 s(16.27%)p 5.12(83.38%)d 0.02(0.29%)
(65.29%) 0.8080* O 8 s(17.13%)p 4.81(82.40%)d 0.03(0.44%)
22. (1.98748) BD (1) C 3- C 4
(52.05%) 0.7215* C 3 s(29.25%)p 2.41(70.56%)d 0.01(0.17%)
(47.95%) 0.6924* C 4 s(35.91%)p 1.78(63.95%)d 0.00(0.11%)
23. (1.95943) BD (1) C 3- O 8
(35.44%) 0.5953* C 3 s(15.92%)p 5.26(83.73%)d 0.02(0.30%)
(64.56%) 0.8035* O 8 s(14.57%)p 5.83(84.95%)d 0.03(0.45%)
25. (1.98990) BD (1) C 4- O 5
(32.33%) 0.5686* C 4 s(27.35%)p 2.65(72.43%)d 0.01(0.16%)
(67.67%) 0.8226* O 5 s(28.90%)p 2.45(70.74%)d 0.01(0.34%)
26. (1.99550) BD (1) C 4- O 6
(35.90%) 0.5992* C 4 s(36.55%)p 1.73(63.32%)d 0.00(0.08%)
(64.10%) 0.8006* O 6 s(39.85%)p 1.49(59.40%)d 0.02(0.68%)
27. (1.98692) BD (2) C 4- O 6
(31.38%) 0.5601* C 4 s(0.21%)p99.99(99.55%)d 0.68(0.14%)
(68.62%) 0.8284* O 6 s(0.22%)p99.99(99.33%)d 1.98(0.43%)
43. (0.21136) BD*(2) C 4- O 6
(68.62%) 0.8284* C 4 s(0.21%)p99.99(99.55%)d 0.68(0.14%)
(31.38%) -0.5601* O 6 s(0.22%)p99.99(99.33%)d 1.98(0.43%)

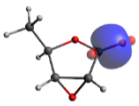

σ(C4-O6)
−30.3 eV
C4: 35.8%
O6:
64.0%

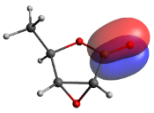

π(C4-O6)
−11.1 eV
P: 31.2%
C: 68.1%

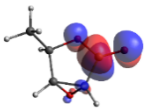

π*(C4-O6)
1.1 eV
s: 68.6%
p: 31.4%

Figure S3. Relevant NLMOs of GVLO (B3LYP/aug-cc-pvtz//B3LYP-D3/def2-TZVP).

The Fukui function is defined as (eq. 1).[10]

$$f(\boldsymbol{r}) = \left[\frac{\partial \rho(\boldsymbol{r})}{\partial N}\right]_v \qquad \text{(eq. 1)}$$

$\rho(\boldsymbol{r})$ is the electron density and N the number of electrons in the system at a fixed external potential v. Using the finite difference approximation, Fukui functions for nucleophilic as well as electrophilic attack can be calculated:

Nucleophilic attack: $f^+(\boldsymbol{r}) = \rho_{N+1}(\boldsymbol{r}) - \rho_N(\boldsymbol{r})$ (eq. 2)
Electrophilic attack: $f^-(\boldsymbol{r}) = \rho_N(\boldsymbol{r}) - \rho_{N-1}(\boldsymbol{r})$ (eq. 3)

The dual-descriptor is closely related to Fukui functions and another useful tool to reveal reactive sites.[11] It can be formulated as follows:

$$\Delta f(\boldsymbol{r}) = f^+(\boldsymbol{r}) - f^-(\boldsymbol{r})$$
$$\Delta f(\boldsymbol{r}) = \rho_{N+1}(\boldsymbol{r}) - 2\rho_N(\boldsymbol{r}) + \rho_{N-1}(\boldsymbol{r}) \qquad \text{(eq. 4)}$$

The electron density was calculated at the B3LYP-D3/6-31G(d) level of theory for the neutral, cationic and anionic species. For the cation and anion the single-point calculation were performed at a fixed geometry (vertical) as the potential is a constant in the partial derivative of the Fukui function. With the aid of MultiWfn 3.6, Gaussian16 formatted checkpoint files were converted into .wfn files and then subtracted to obtain $f^+(\boldsymbol{r})$ and the dual descriptor $\Delta f(\boldsymbol{r})$ and to plot the corresponding isosurfaces according to eq. 2 and eq. 4. The $f^+(\boldsymbol{r})$ function clearly shows that a nucleophilic attack is favored at the lactone carbonyl carbon (C4). This is further supported by $\Delta f(\boldsymbol{r})$ revealing C4 (green isosurface) as the site where nucleophiles attack. The lactone carbonyl atom has a large positive condensed (Hirshfeld) Fukui index $f_k{}^+$ of 0.194, compared to those of the epoxide C atoms (C2: 0.060; C3: 0.086) which agrees well with the nucleophilic attack being observed solely on C4. The quantified values for f+, f− and the dual descriptor Δf are summarized in Table S3.

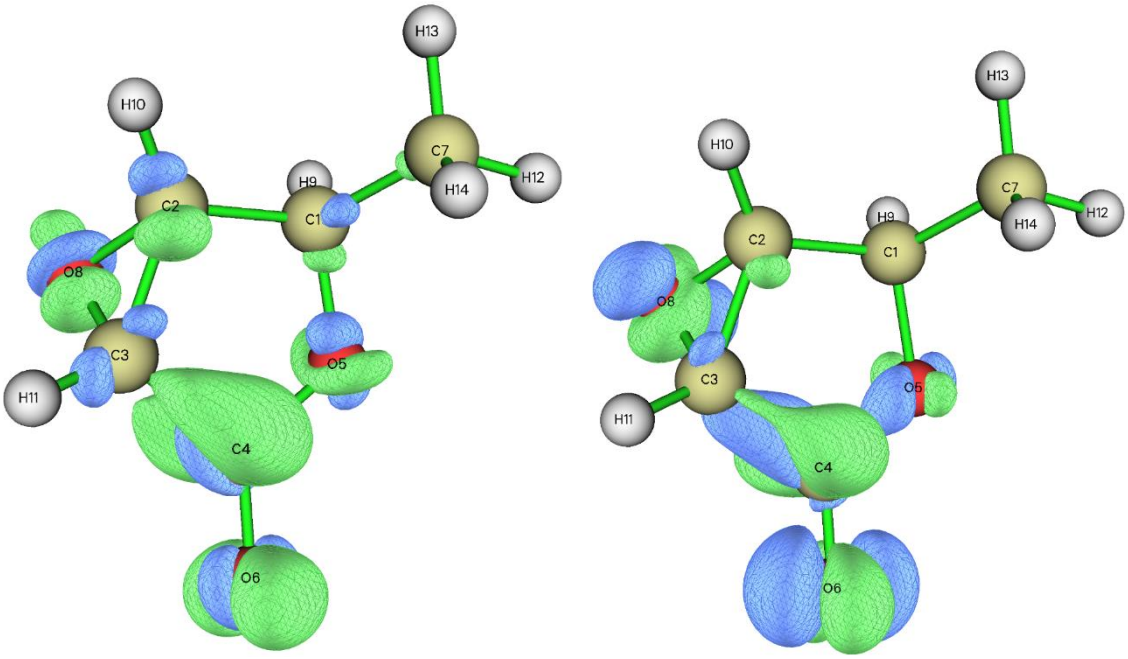

Figure S4. Isosurface of the $f^+(r)$ function (left) and the dual descriptor $\Delta f(r)$ (right) of GVLO (isosurface value = 0.01; green denotes positive $f^+(r)$ and $\Delta f(r)$ values and thus nucleophilic sites).

Table S3. Calculated Hirshfeld-Charges at the B3LYP-D3/6-31G(d) level of theory and quantitative values for f^+, f and the dual descriptor Δf.

Atom	q_N^{Hirsch}	q_{anion}^{Hirsch}	q_{cation}^{Hirsch}	f^-	f^+	Δf
C1	0.0654	0.0402	0.0943	0.0289	0.0252	-0.0036
C2	0.0340	-0.0264	0.0998	0.0658	0.0604	-0.0054
C3	0.0334	-0.0526	0.1038	0.0703	0.0860	0.0157
C4	0.2052	0.0112	0.2834	0.0783	0.1940	0.1157

Optimized structures (.xyz-files)

GVLO

```
14
GVLO @ B3LYP-D3/def2-TZVP
C          1.14168       -0.08638       -0.42569
C          0.55474        1.13937        0.23896
C         -0.83969        0.83866        0.55381
C         -1.09820       -0.55505        0.04985
O          0.01477       -0.98546       -0.60277
O         -2.08168       -1.22012        0.17987
C          2.20689       -0.76602        0.40847
O         -0.49332        1.72774       -0.52241
H          1.50899        0.15058       -1.42576
H          1.17445        1.81075        0.82080
H         -1.42158        1.24718        1.36769
H          2.50492       -1.70561       -0.05478
H          3.08681       -0.12466        0.48950
H          1.83583       -0.97895        1.41270
```

Crystallographic data

X-ray structure determination X-ray quality crystals were selected in Fomblin YR-1800 perfluoroether (Alfa Aesar) at ambient temperature. The sample was cooled to 250(2) K during measurement, as cooling to lower temperatures resulted in cracking of the crystals in the cryo-stream. The data were collected on a Bruker Apex II Duo diffractometer using CuK_α radiation (λ = 1.54178 Å). The structure was solved by direct methods (SHELXS)[12] and refined by full matrix least squares procedures (SHELXL).[13] Semi-empirical absorption corrections (multi-scan and additional spherical absorption correction) were applied to the diffraction data using the SADABS application within the APEX II platform.[14] All non-hydrogen atoms were refined anisotropically, hydrogen atoms were included in the refinement at calculated positions using a riding model (except H1A and H3, which were identified in the Difference Fourier Map).

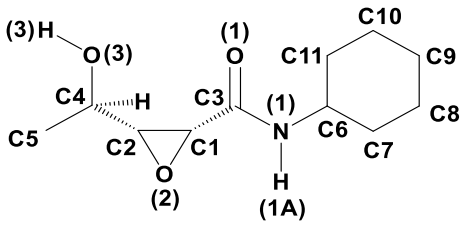

Scheme S1. Numbering scheme of $C_{11}H_{19}NO_3$.

Table S4. Selected bond lengths (Å) and angles (°) of $C_{11}H_{19}NO_3$.

Bond	Bond lengths (Å)	Bond	Bond length (Å)
C1–O2	1.4358(16)	**C1–C3**	1.4986(17)
C1–C2	1.4702(17)	**C3–N1**	1.3239(15)
C2–O2	1.4430(14)	**C3–O1**	1.2338(15)
N1–C6	1.4620(15)	**C2–C4**	1.5033(16)
C4–O3	1.4230(14)		
Angle	**Bond angle (°)**	**Angle**	**Bond angle (°)**
O1–C3–C1	119.02(11)	**N1–C3–O1**	124.35(11)
C2–O1–C1	61.42(8)	**C3–N1–C6**	123.41(10)
C6–N1–H1A	118.0(10)	**C3–N1–H1A**	118.5(10)
C1–C3–N1	116.62(11)		

Table S5. X-ray analysis of $C_{11}H_{19}NO_3$.

Data	**$C_{11}H_{19}NO_3$**
Empirical formula	$C_{11}H_{19}NO_3$
Formula weight	213.27
Temperature/K	250(2)
Crystal system	monoclinic
Space group	$P2_1/c$
a/Å	11.3947(2)
b/Å	8.8485(2)
c/Å	12.0913(2)
α/°	90
β/°	107.8193(7)
γ/°	90
Volume/Å^3	1160.63(4)
Z	4
ρ_{calc}g/cm^3	1.221
μ/mm^{-1}	0.719
F(000)	464
Crystal size/mm^3	0.26 × 0.19 × 0.10
Radiation	CuKα (λ = 1.54178)
2*Θ* range for data collection/°	8.150 to 133.162
Index ranges	-13 ≤ h ≤ 13, -10 ≤ k ≤ 10, -14 ≤ l ≤ 14
Reflections collected	12257
Independent reflections	2057 [R_{int} = 0.0221, R_{sigma} = 0.0148]
Data/restraints/parameters	2057/0/145
Goodness-of-fit on F^2	1.059
Final R indexes [I>=2σ (I)]	R_1 = 0.0389, wR_2 = 0.1020
Final R indexes [all data]	R_1 = 0.0398, wR_2 = 0.1032
Largest diff. peak/hole / e Å^{-3}	0.19/-0.19
CCDC #	2256162

NMR and IR spectra

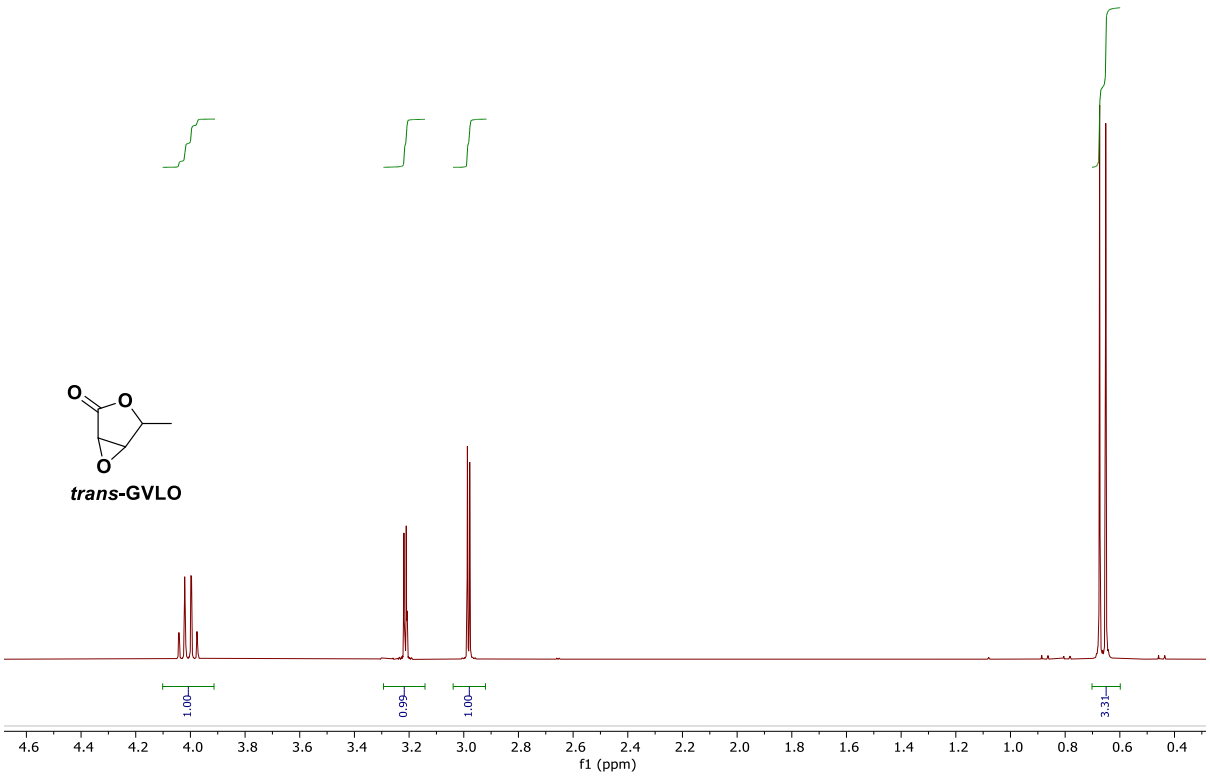

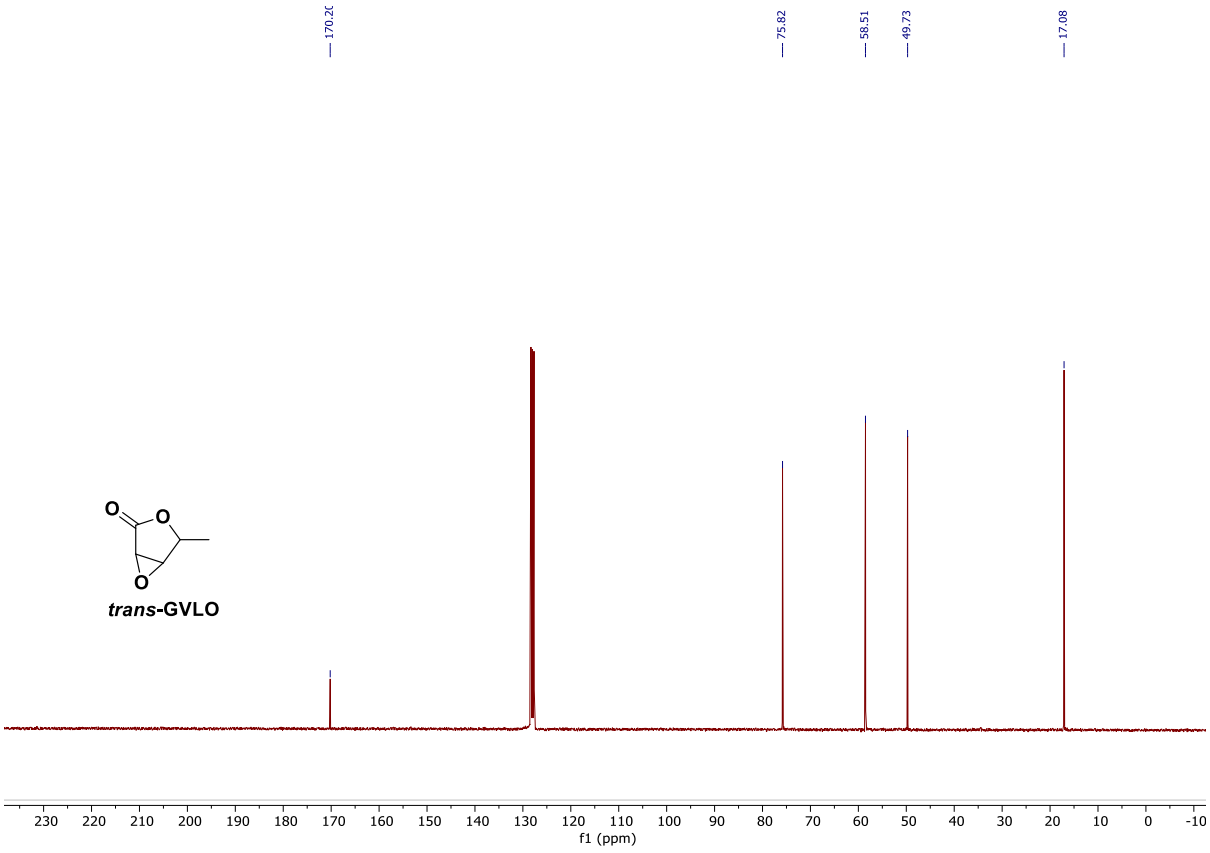

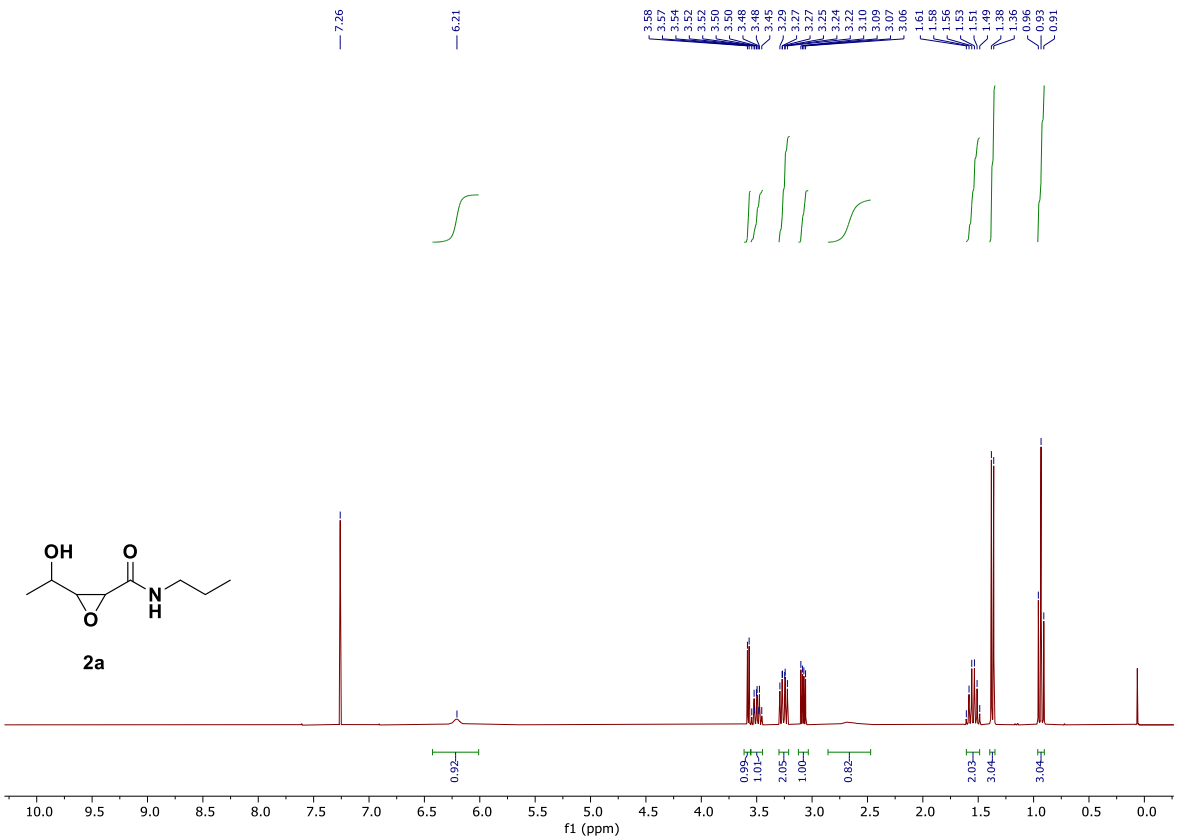
7.26
6.21
3.58
3.57
3.54
3.52
3.50
3.48
3.45
3.29
3.27
3.25
3.24
3.22
3.10
3.09
3.07
3.06
1.61
1.58
1.56
1.53
1.51
1.49
1.38
1.36
0.96
0.93
0.91
OH
O
N
H
O
2a
0.92
0.99
1.01
2.05
1.00
0.82
2.03
3.04
3.04
10.0
9.5
9.0
8.5
8.0
7.5
7.0
6.5
6.0
5.5
5.0
4.5
4.0
3.5
3.0
2.5
2.0
1.5
1.0
0.5
0.0
f1 (ppm)

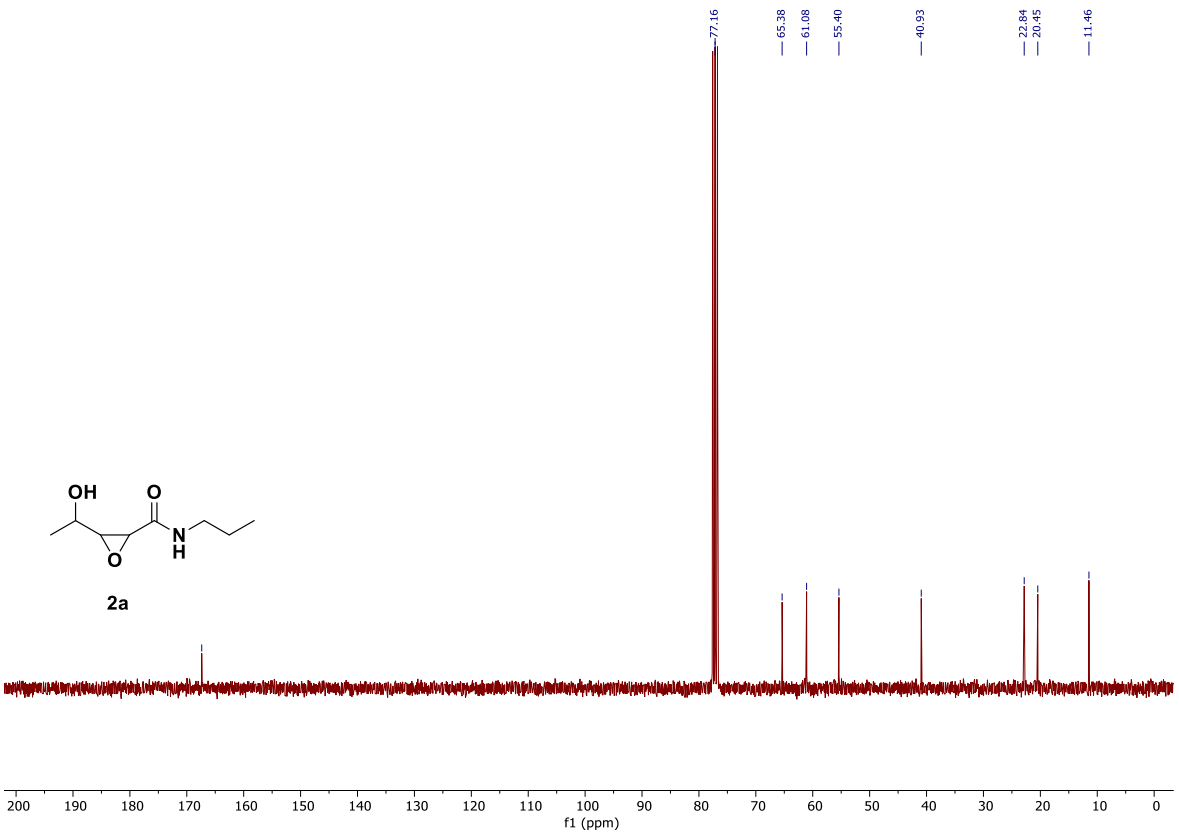
77.16
65.38
61.08
55.40
40.93
22.84
20.45
11.46
OH
O
N
H
O
2a
200
190
180
170
160
150
140
130
120
110
100
90
80
70
60
50
40
30
20
10
0
f1 (ppm)

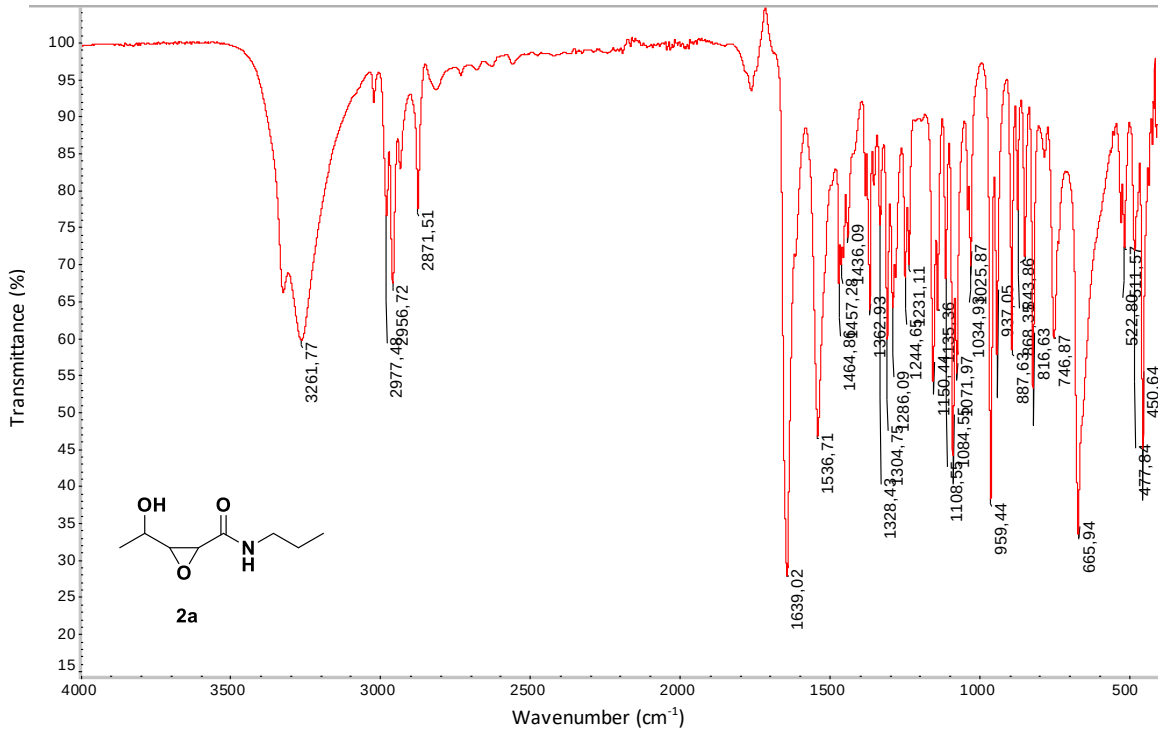
Transmittance (%)
Wavenumber (cm-1)
3261,77
2977,48
2956,72
2871,51
1639,02
1536,71
1464,96
1457,28
1436,09
1362,93
1328,43
1304,75
1286,09
1244,65
1231,11
1150,44
1135,36
1108,55
1084,55
1071,97
1034,98
1025,87
959,44
937,05
887,63
868,35
843,86
816,63
746,87
665,94
522,80
511,57
477,64
450,64
OH
O
N
H
O
2a

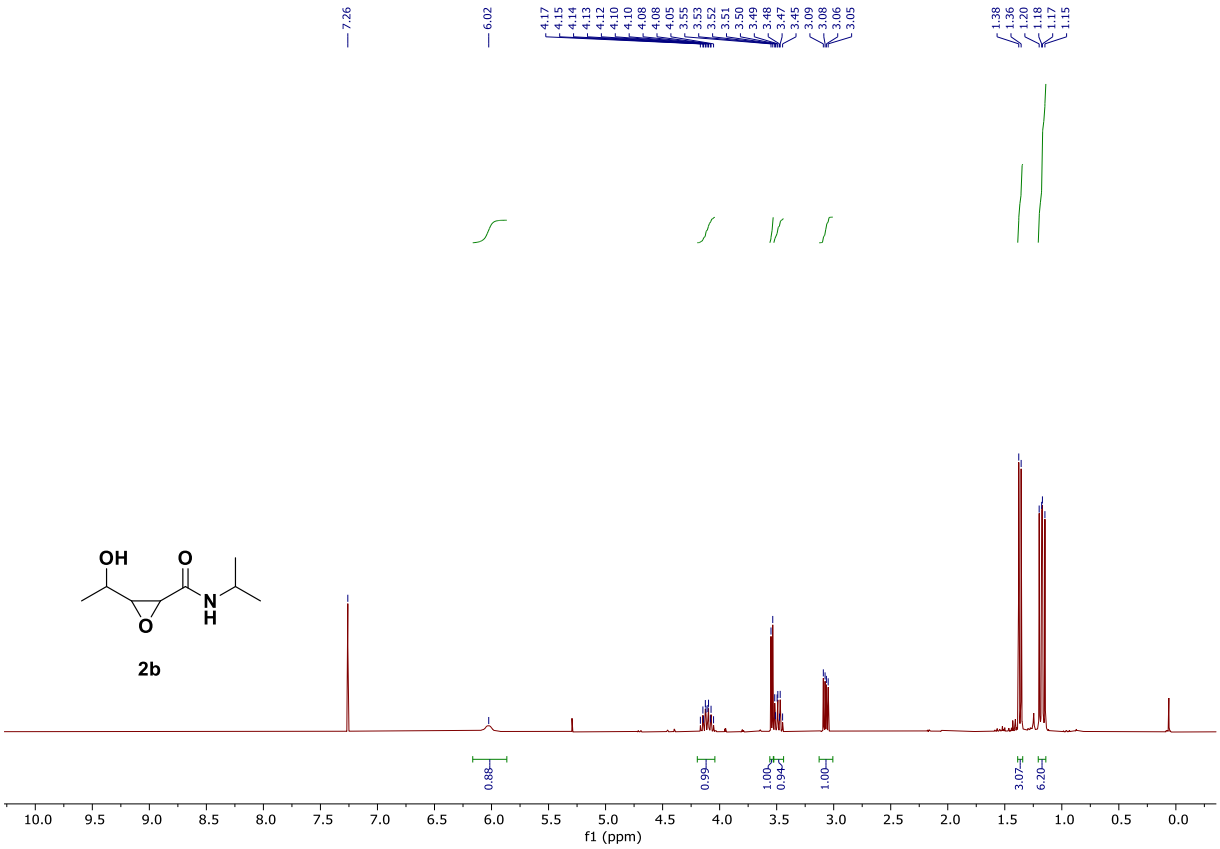
7.26
6.02
4.17
4.15
4.14
4.13
4.12
4.10
4.10
4.08
4.08
4.05
3.55
3.53
3.52
3.51
3.50
3.49
3.48
3.47
3.45
3.09
3.08
3.06
3.05
1.38
1.36
1.20
1.18
1.17
1.15
0.88
0.99
1.00
0.94
1.00
3.07
6.20
f1 (ppm)
OH
O
N
H
O
2b

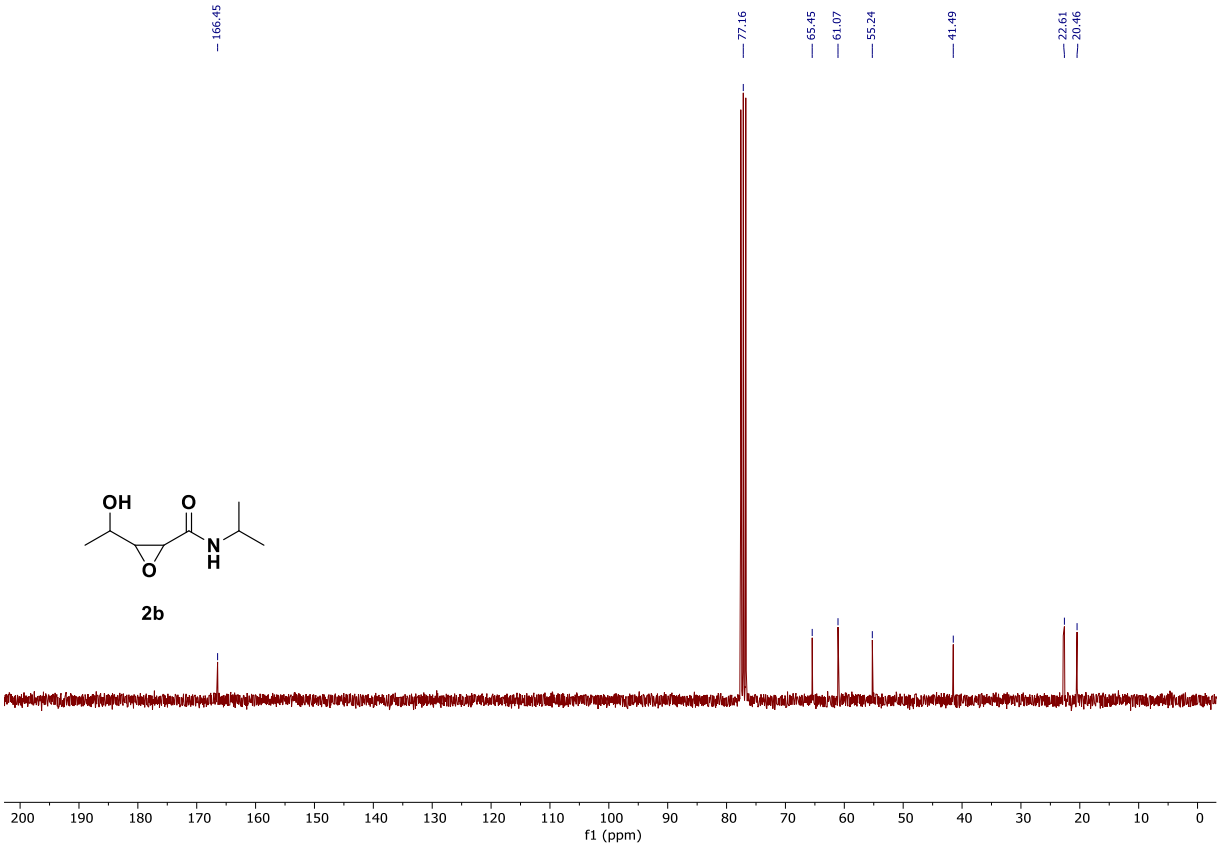
166.45
77.16
65.45
61.07
55.24
41.49
22.61
20.46
OH
O
N
H
O
2b
f1 (ppm)

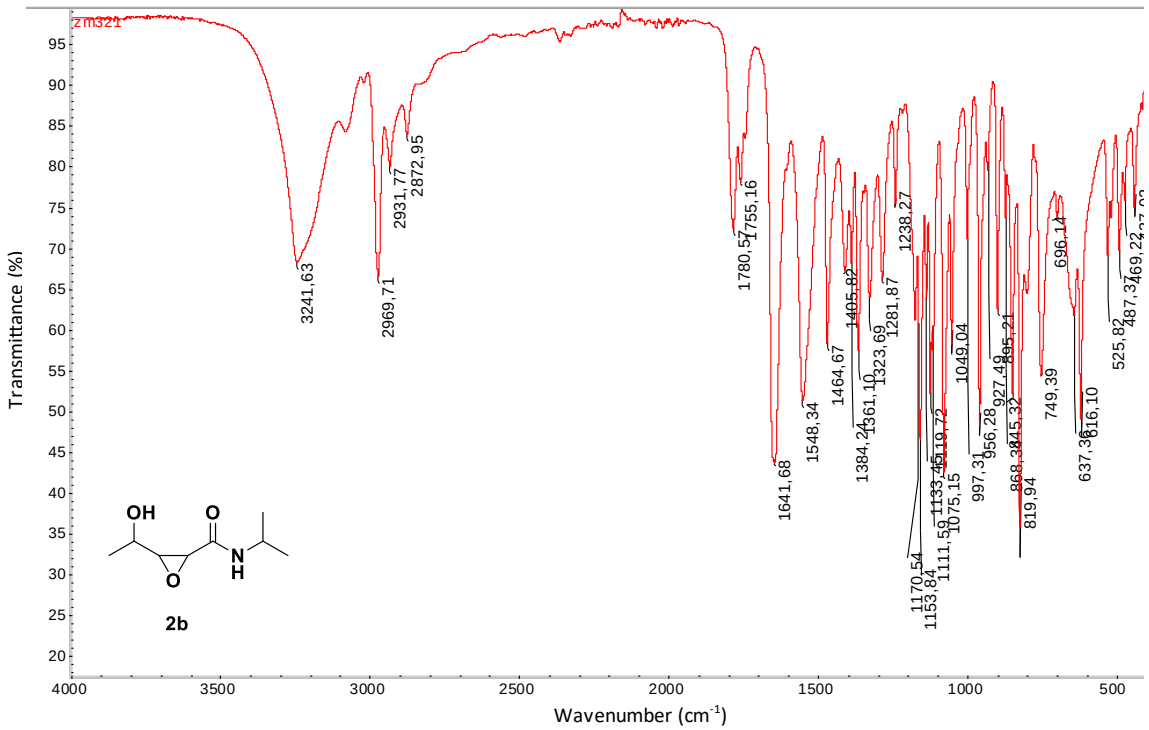
zm321
Transmittance (%)
Wavenumber (cm-1)
3241,63
2969,71
2931,77
2872,95
1780,57
1755,16
1641,68
1548,34
1464,67
1405,82
1384,24
1361,10
1323,69
1281,87
1238,27
1170,54
1153,84
1111,58
1075,15
1049,04
997,31
956,28
927,48
895,21
868,38
845,32
819,94
749,39
696,14
637,36
616,10
525,82
487,37
469,22
OH
O
N
H
O
2b

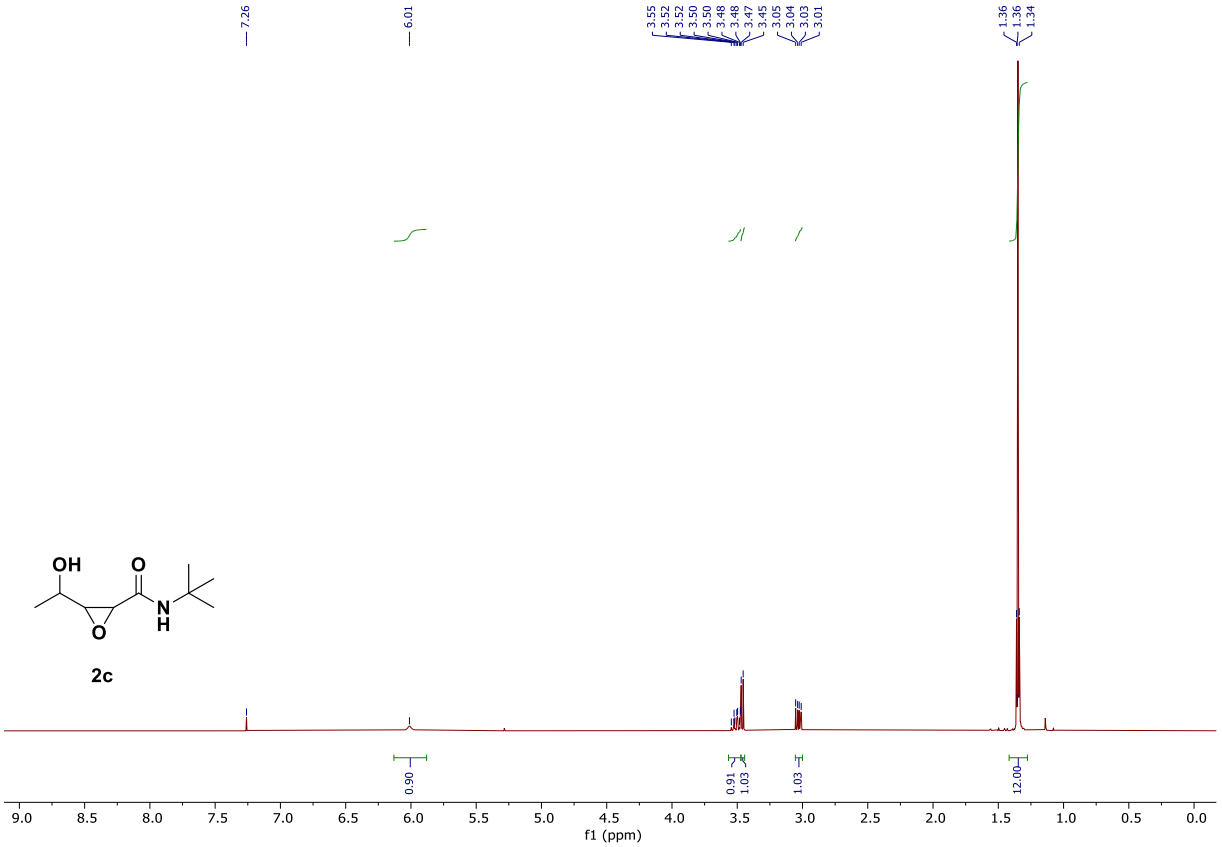
7.26
6.01
3.55
3.52
3.52
3.50
3.50
3.48
3.48
3.47
3.45
3.05
3.04
3.03
3.01
1.36
1.36
1.34
OH
O
N
H
O
2c
0.90
0.91
1.03
1.03
12.00
9.0
8.5
8.0
7.5
7.0
6.5
6.0
5.5
5.0
4.5
4.0
3.5
3.0
2.5
2.0
1.5
1.0
0.5
0.0
f1 (ppm)

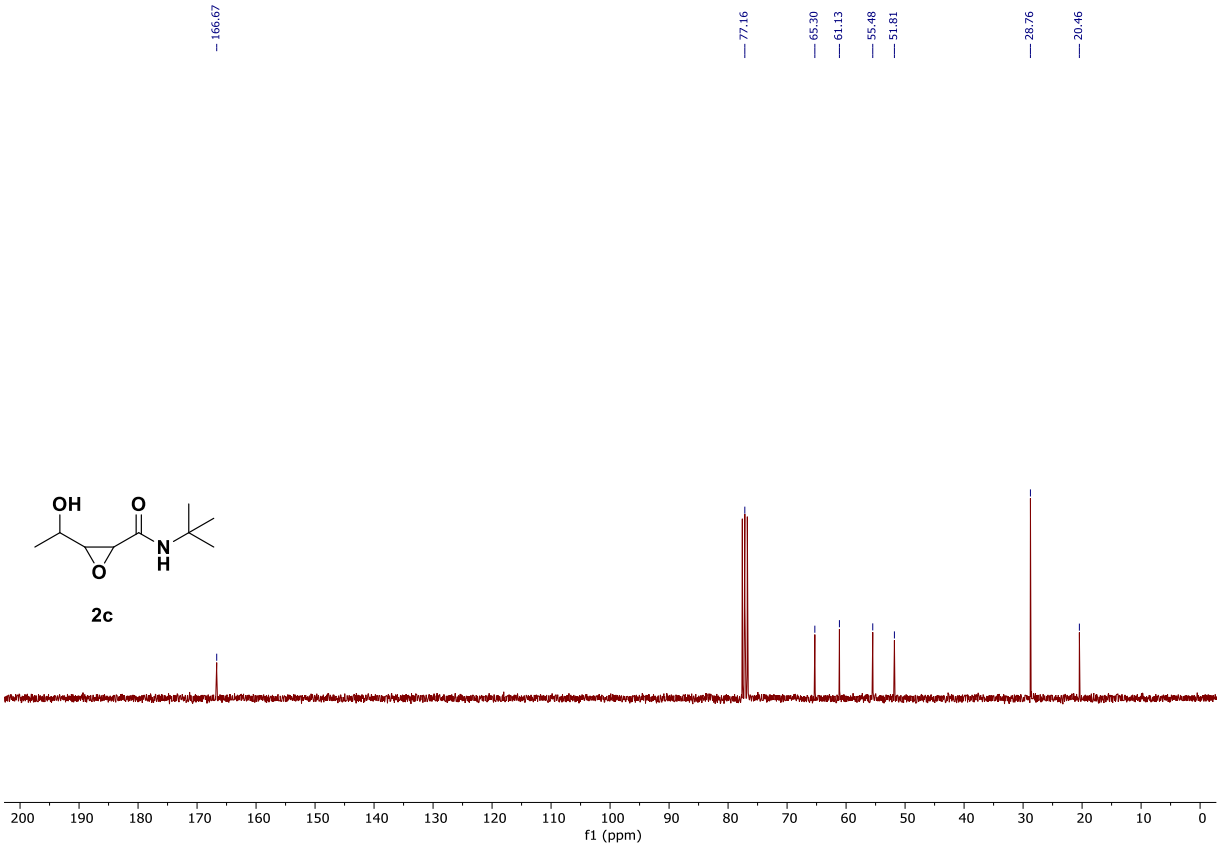
166.67
77.16
65.30
61.13
55.48
51.81
28.76
20.46
OH
O
N
H
O
2c
200
190
180
170
160
150
140
130
120
110
100
90
80
70
60
50
40
30
20
10
0
f1 (ppm)

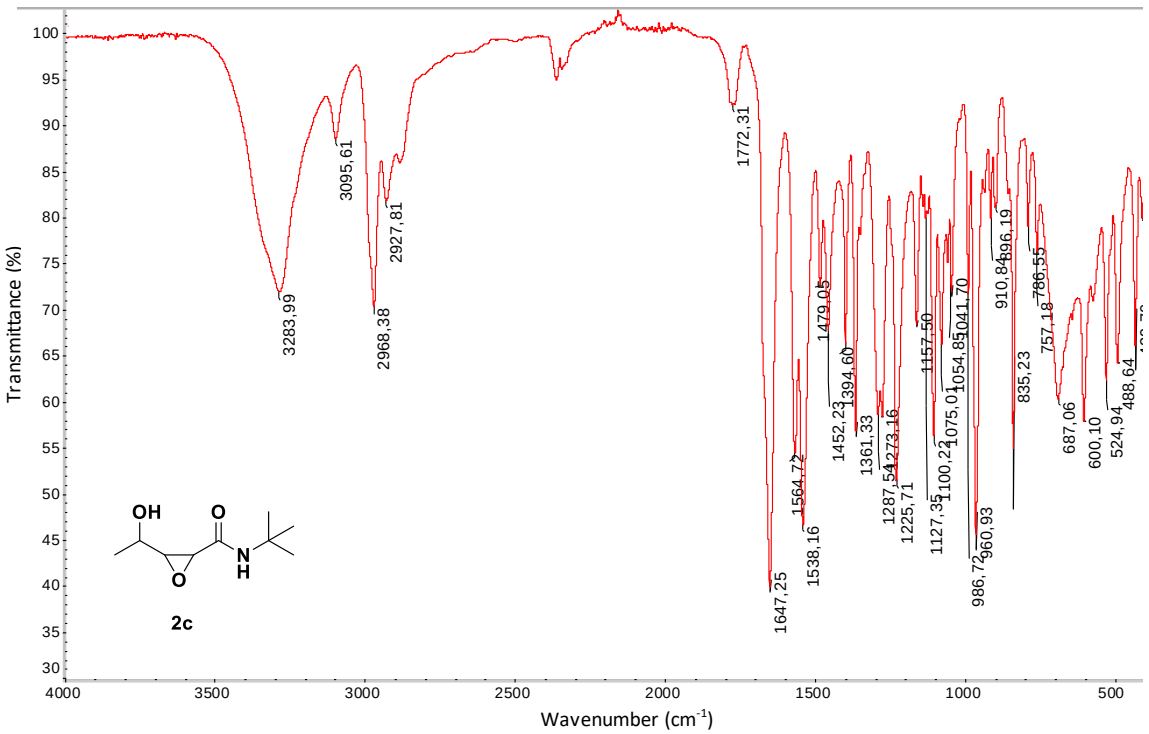
Transmittance (%)
Wavenumber (cm-1)
3283,99
3095,61
2968,38
2927,81
1772,31
1647,25
1564,72
1538,16
1479,05
1452,23
1394,60
1361,33
1287,54
1273,16
1225,71
1157,50
1127,35
1100,22
1075,01
1054,85
1041,70
986,72
960,93
910,84
896,19
835,23
786,55
757,18
687,06
600,10
524,94
488,64
OH
O
N
H
O
2c

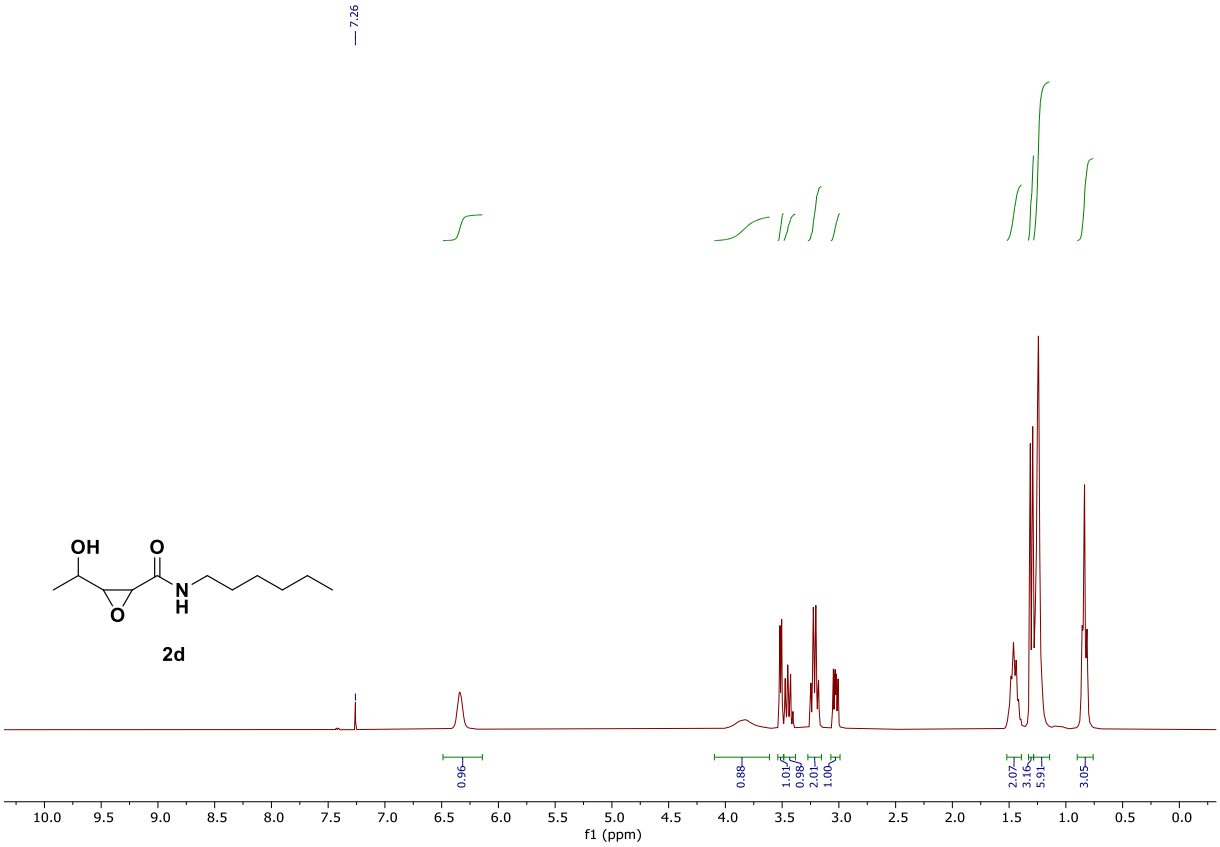
7.26
OH
O
N
H
O
2d
0.96
0.88
1.01
0.98
2.01
1.00
2.07
3.16
5.91
3.05
f1 (ppm)

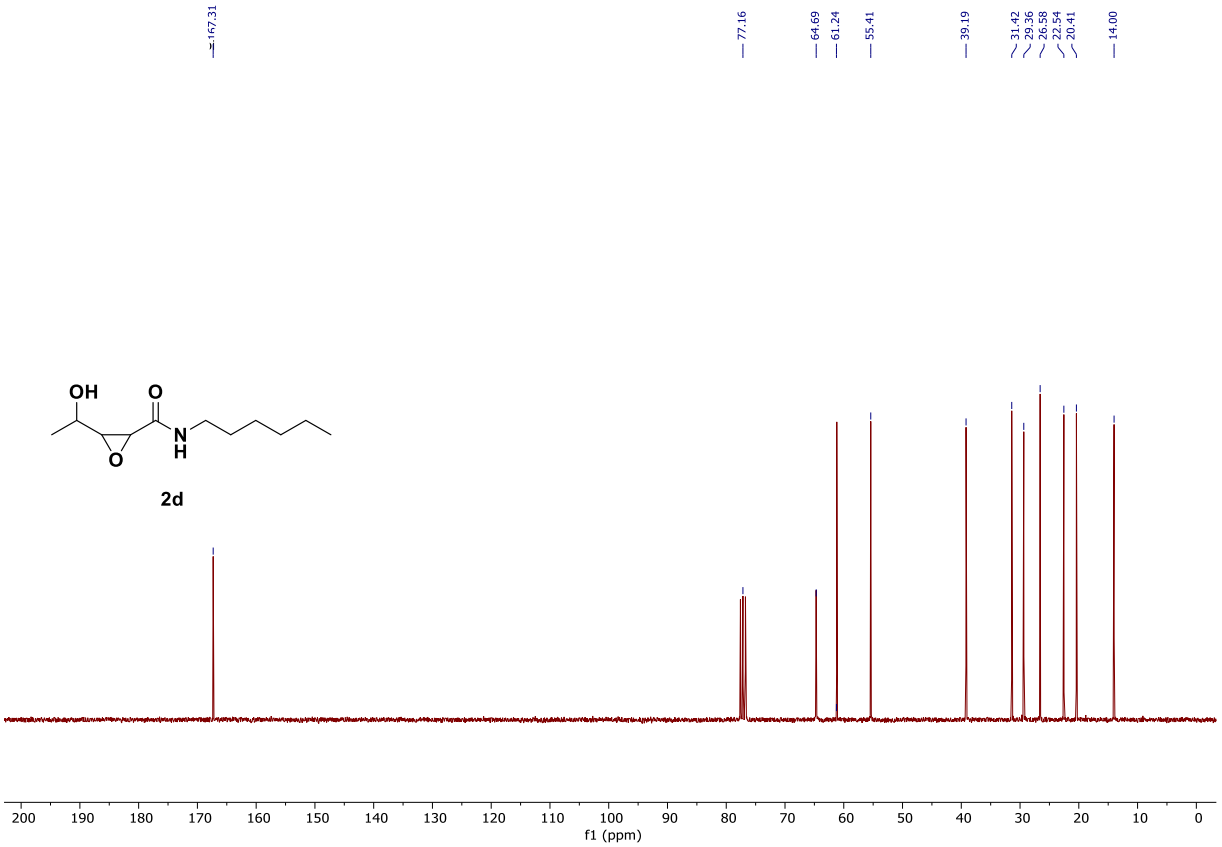
167.31
77.16
64.69
61.24
55.41
39.19
31.42
29.36
26.58
22.54
20.41
14.00
OH
O
N
H
O
2d
200 190 180 170 160 150 140 130 120 110 100 90 80 70 60 50 40 30 20 10 0
f1 (ppm)

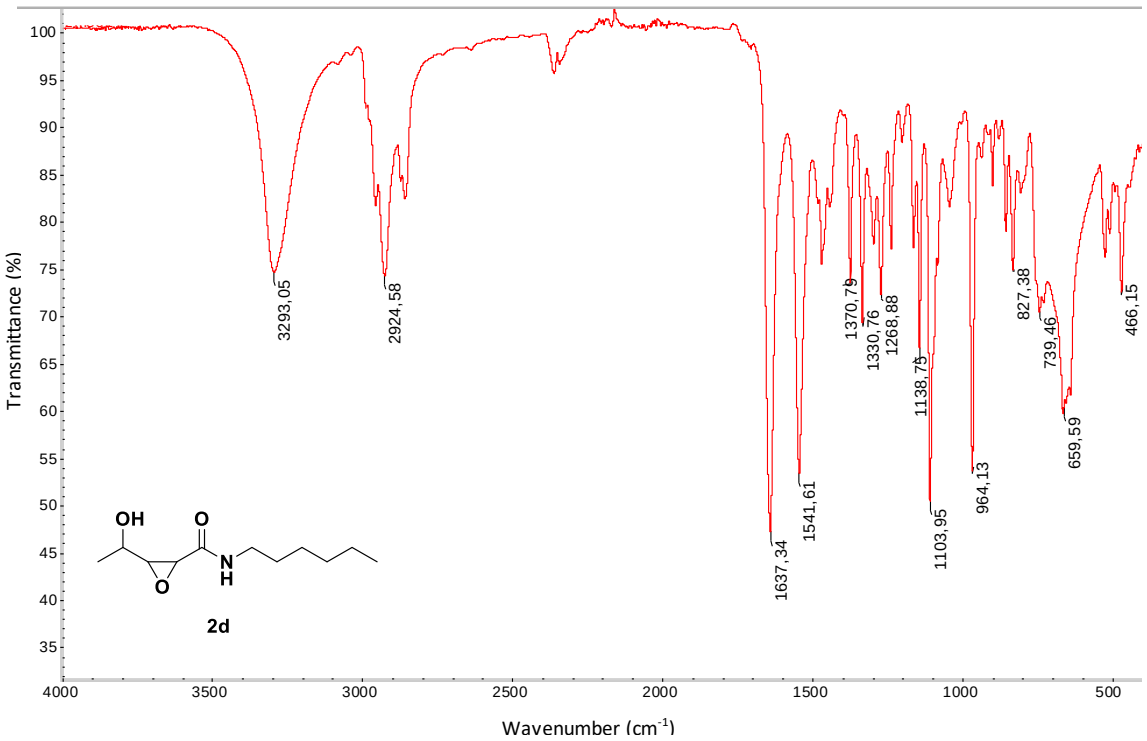
Transmittance (%)
100 95 90 85 80 75 70 65 60 55 50 45 40 35
3293,05
2924,58
1637,34
1541,61
1370,79
1330,76
1268,88
1138,75
1103,95
964,13
827,38
739,46
659,59
466,15
OH
O
N
H
O
2d
4000 3500 3000 2500 2000 1500 1000 500
Wavenumber (cm-1)

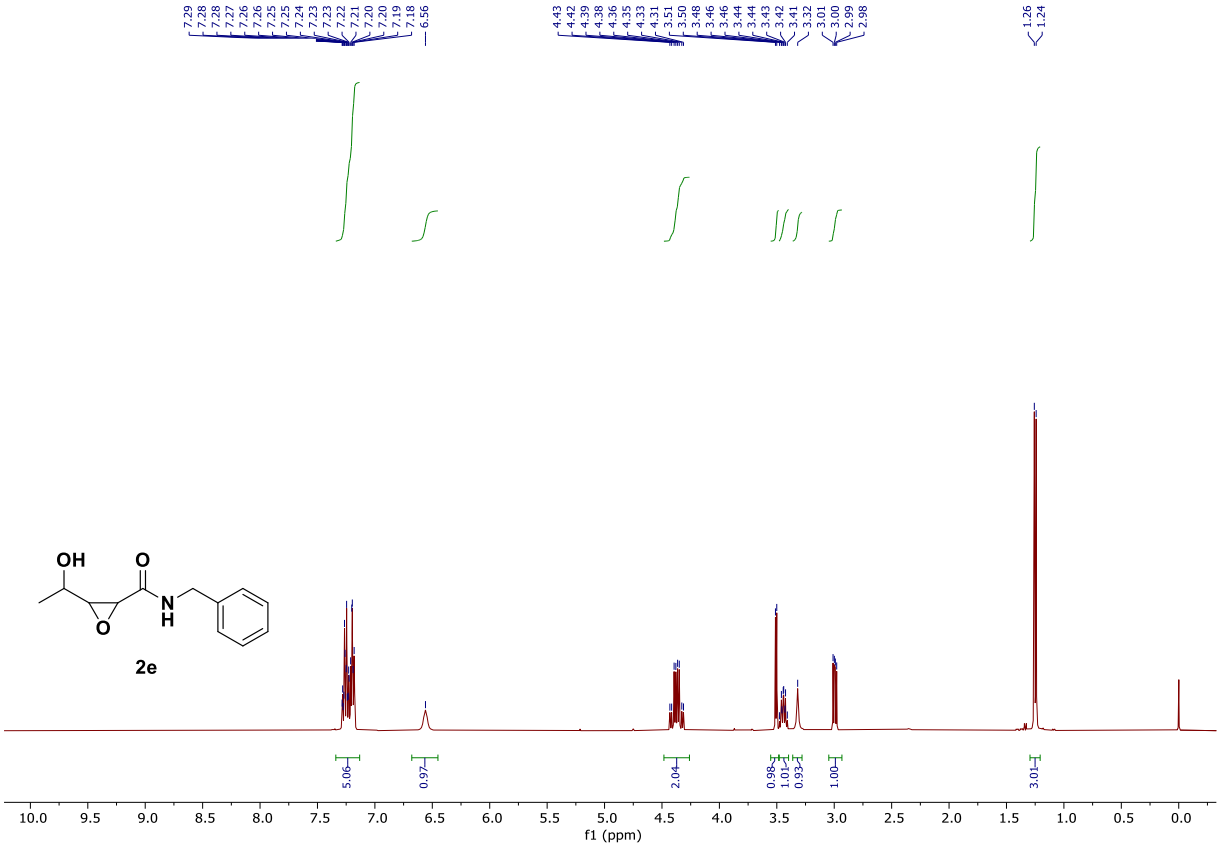
7.29
7.28
7.28
7.27
7.26
7.26
7.25
7.25
7.24
7.23
7.23
7.22
7.21
7.20
7.20
7.19
7.18
6.56
4.43
4.42
4.39
4.38
4.36
4.35
4.33
4.31
3.51
3.50
3.48
3.46
3.46
3.44
3.44
3.43
3.42
3.41
3.32
3.01
3.00
2.99
2.98
1.26
1.24
OH
O
N
H
O
2e
5.06
0.97
2.04
0.98
1.01
0.93
1.00
3.01
10.0
9.5
9.0
8.5
8.0
7.5
7.0
6.5
6.0
5.5
5.0
4.5
4.0
3.5
3.0
2.5
2.0
1.5
1.0
0.5
0.0
f1 (ppm)

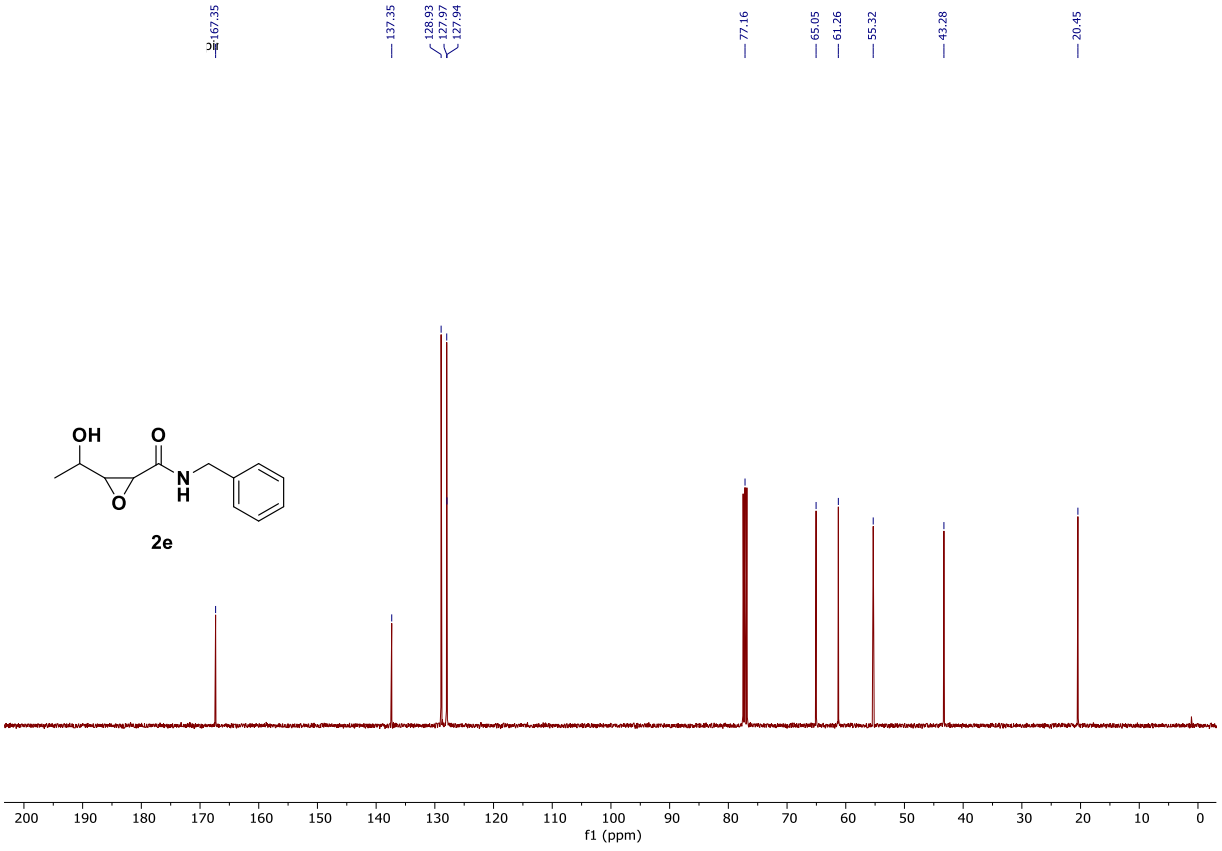
167.35
137.35
128.93
127.97
127.94
77.16
65.05
61.26
55.32
43.28
20.45
OH
O
N
H
O
2e
200
190
180
170
160
150
140
130
120
110
100
90
80
70
60
50
40
30
20
10
0
f1 (ppm)

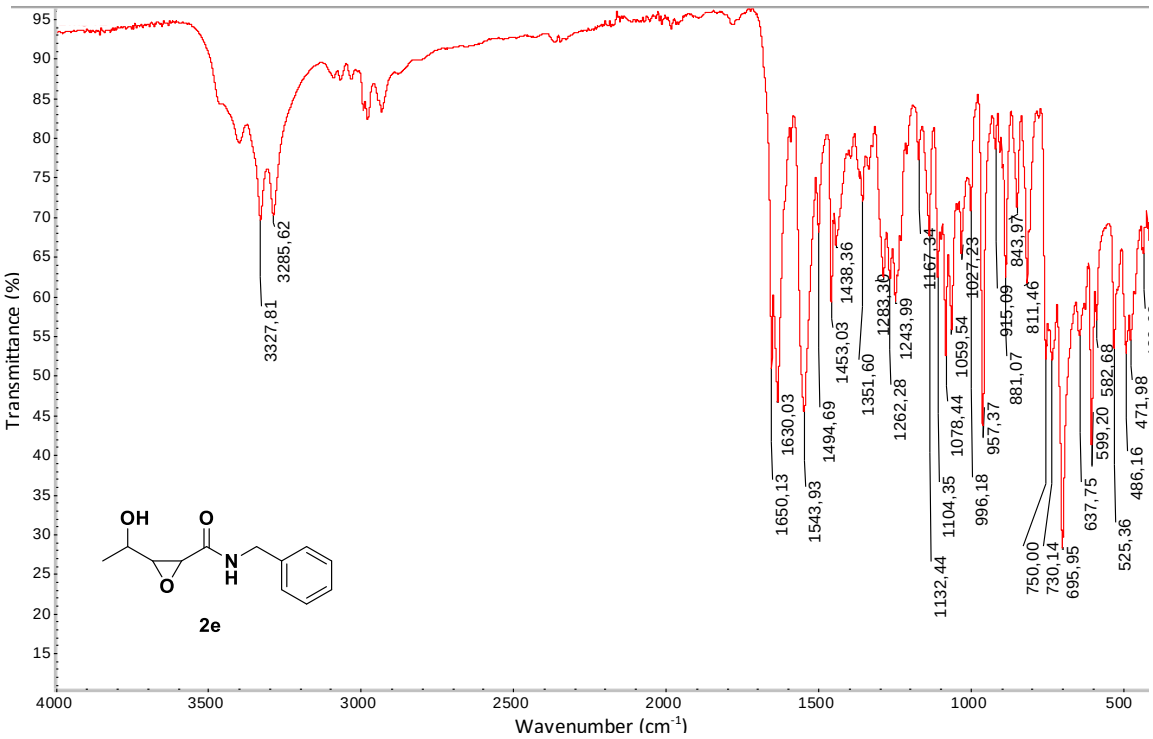
Transmittance (%)
Wavenumber (cm-1)
3327,81
3285,62
1650,13
1630,03
1543,93
1494,69
1453,03
1438,36
1351,60
1283,30
1262,28
1243,99
1167,34
1132,44
1104,35
1078,44
1059,54
1027,23
996,18
957,37
915,09
881,07
843,97
811,46
750,00
730,14
695,95
637,75
599,20
582,68
525,36
486,16
471,98
OH
O
N
H
O
2e

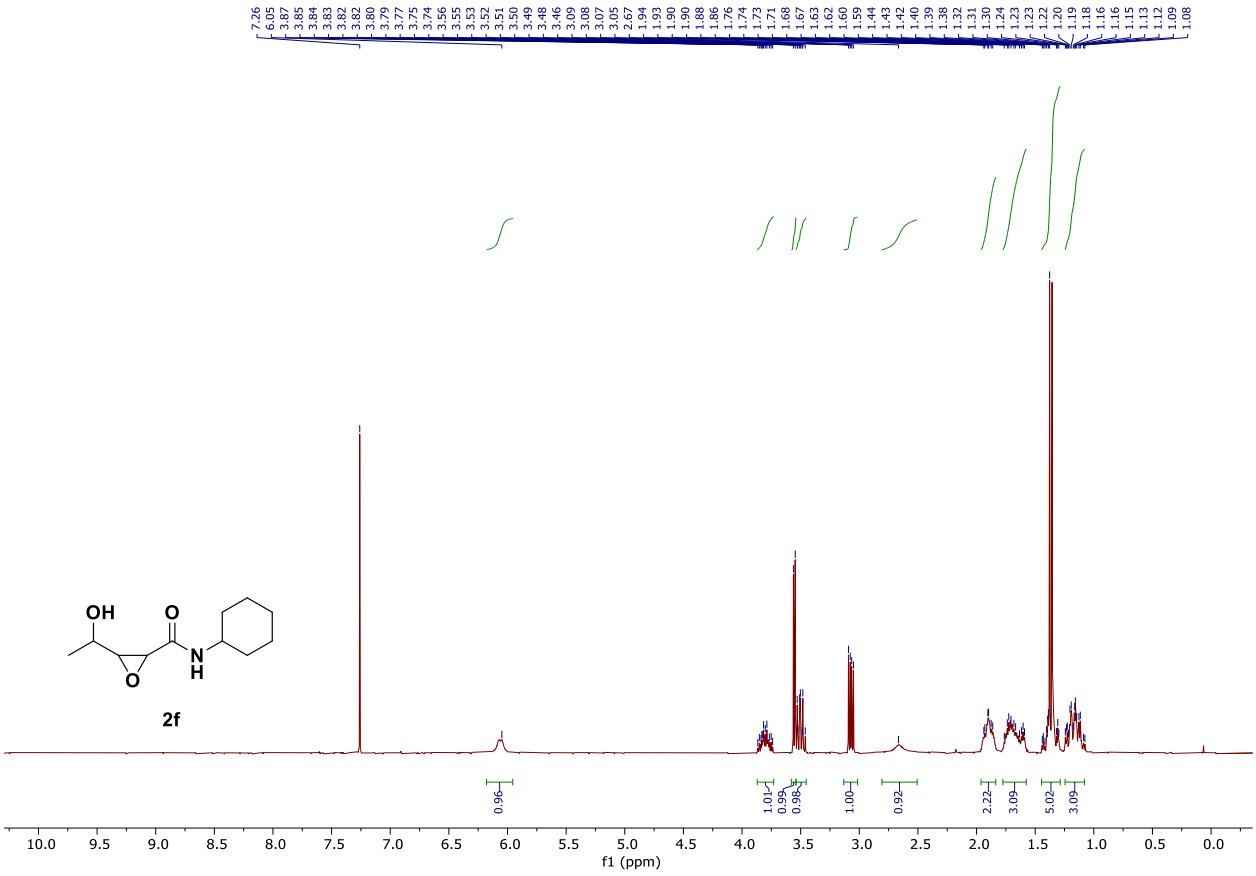
f1 (ppm)
OH
O
N
H
O
2f

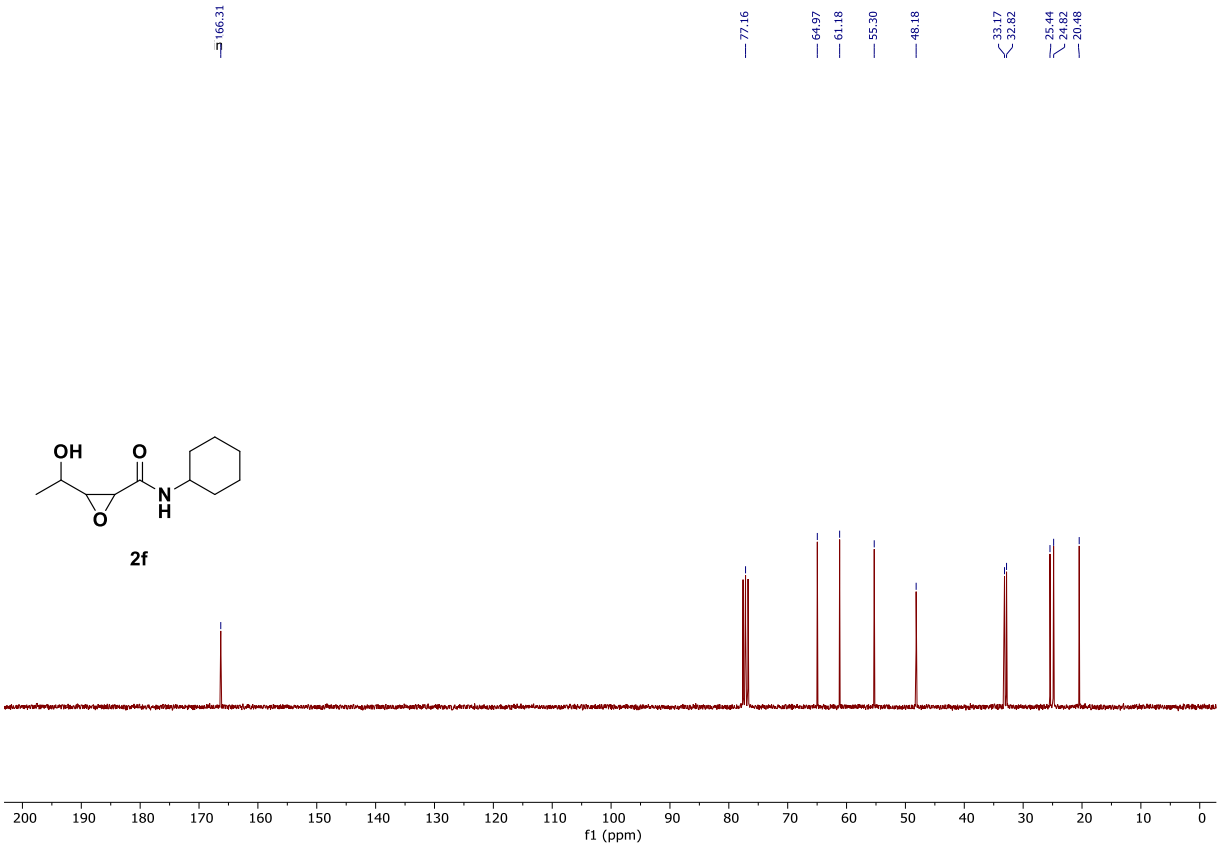
166.31
77.16
64.97
61.18
55.30
48.18
33.17
32.82
25.44
24.82
20.48
OH
O
N
H
O
2f
200 190 180 170 160 150 140 130 120 110 100 90 80 70 60 50 40 30 20 10 0
f1 (ppm)

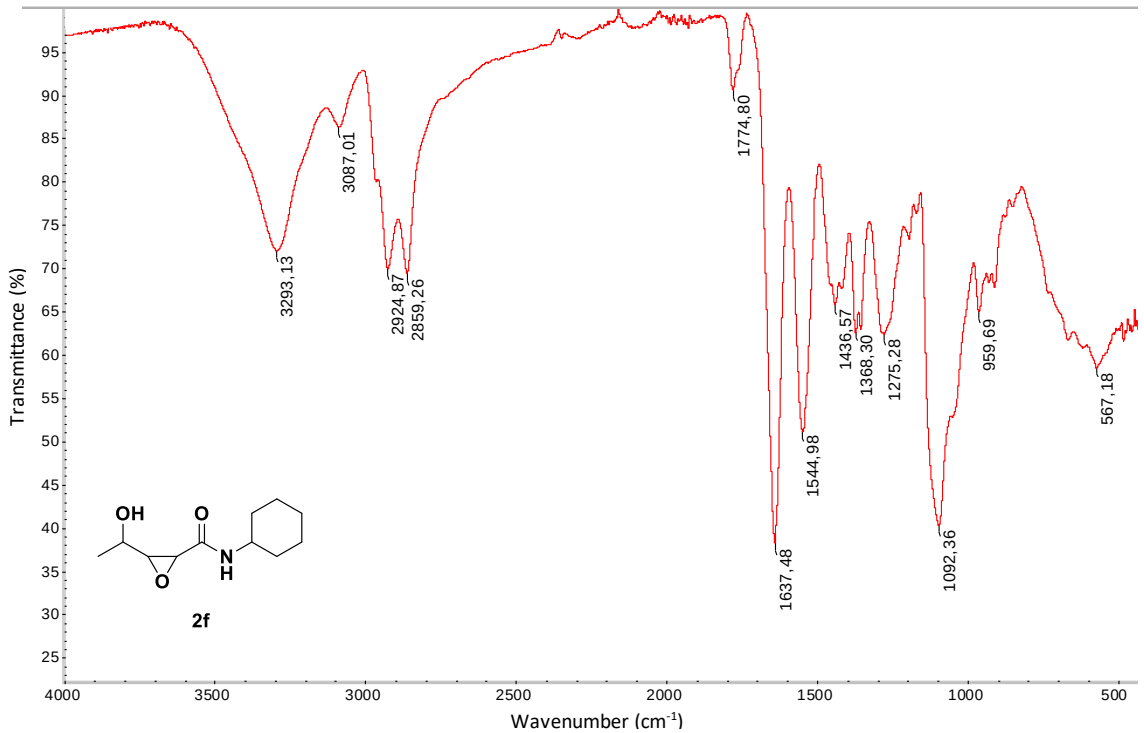
Transmittance (%)
95 90 85 80 75 70 65 60 55 50 45 40 35 30 25
3293,13
3087,01
2924,87
2859,26
1774,80
1637,48
1544,98
1436,57
1368,30
1275,28
1092,36
959,69
567,18
OH
O
N
H
O
2f
4000 3500 3000 2500 2000 1500 1000 500
Wavenumber (cm-1)

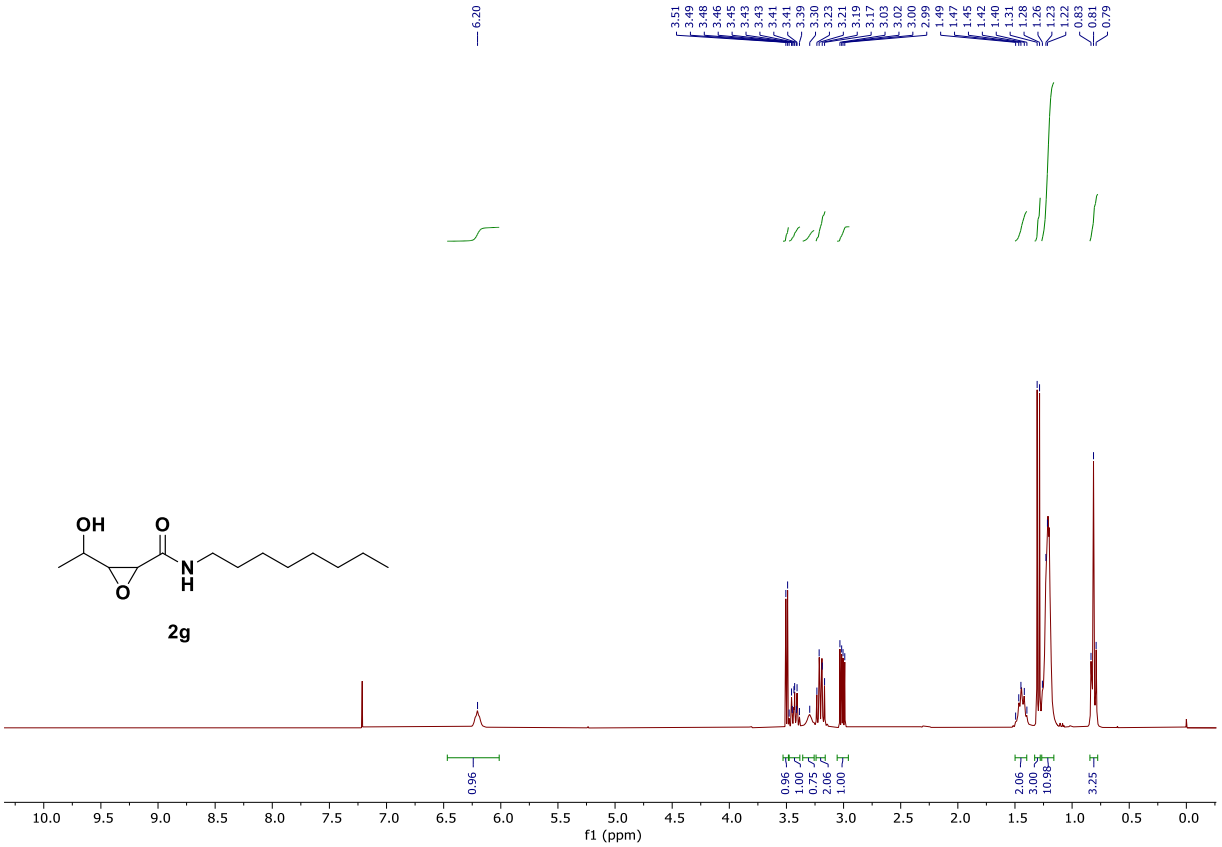
6.20
3.51
3.49
3.48
3.46
3.45
3.43
3.43
3.41
3.41
3.39
3.30
3.23
3.21
3.19
3.17
3.03
3.02
3.00
2.99
1.49
1.47
1.45
1.42
1.40
1.31
1.28
1.26
1.23
1.22
0.83
0.81
0.79
OH
O
N
H
O
2g
0.96
0.96
1.00
0.75
2.06
1.00
2.06
3.00
10.98
3.25
10.0
9.5
9.0
8.5
8.0
7.5
7.0
6.5
6.0
5.5
5.0
4.5
4.0
3.5
3.0
2.5
2.0
1.5
1.0
0.5
0.0
f1 (ppm)

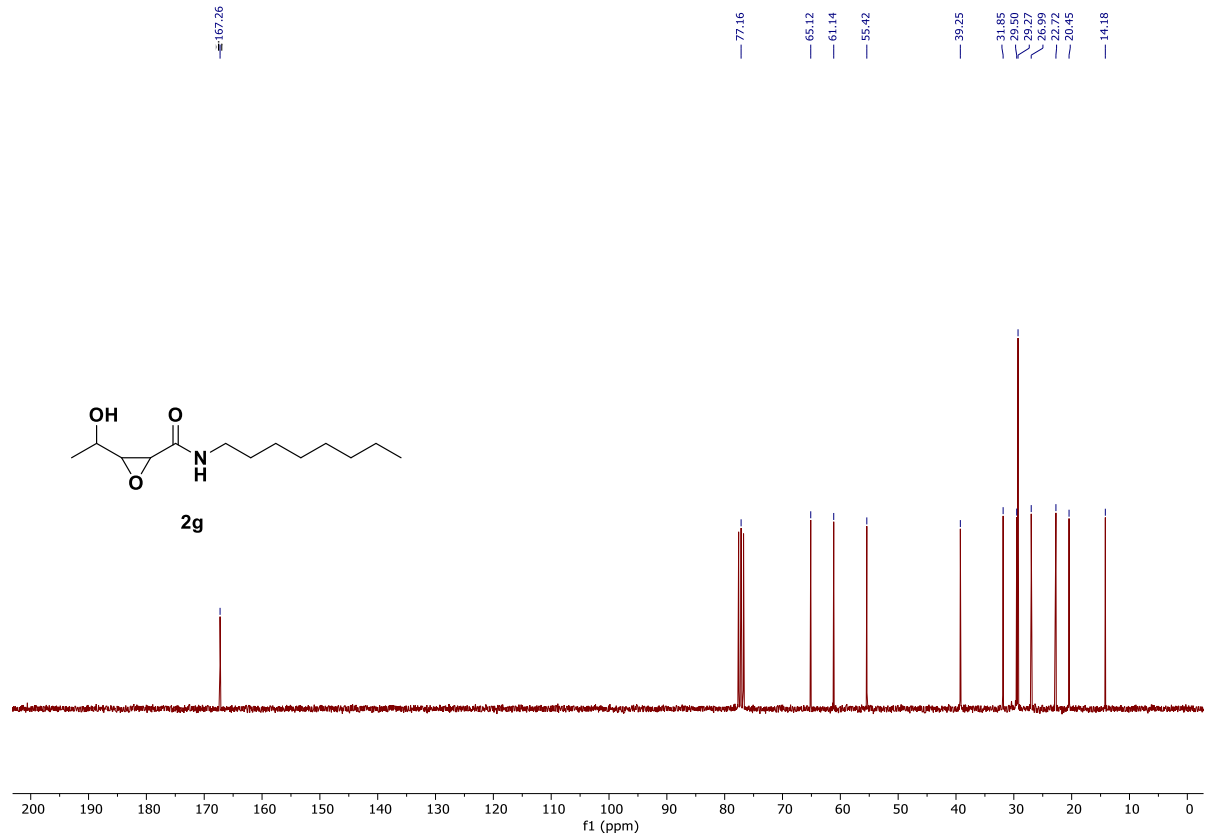
167.26
77.16
65.12
61.14
55.42
39.25
31.85
29.50
29.27
26.99
22.72
20.45
14.18
OH
O
N
H
O
2g
200
190
180
170
160
150
140
130
120
110
100
90
80
70
60
50
40
30
20
10
0
f1 (ppm)

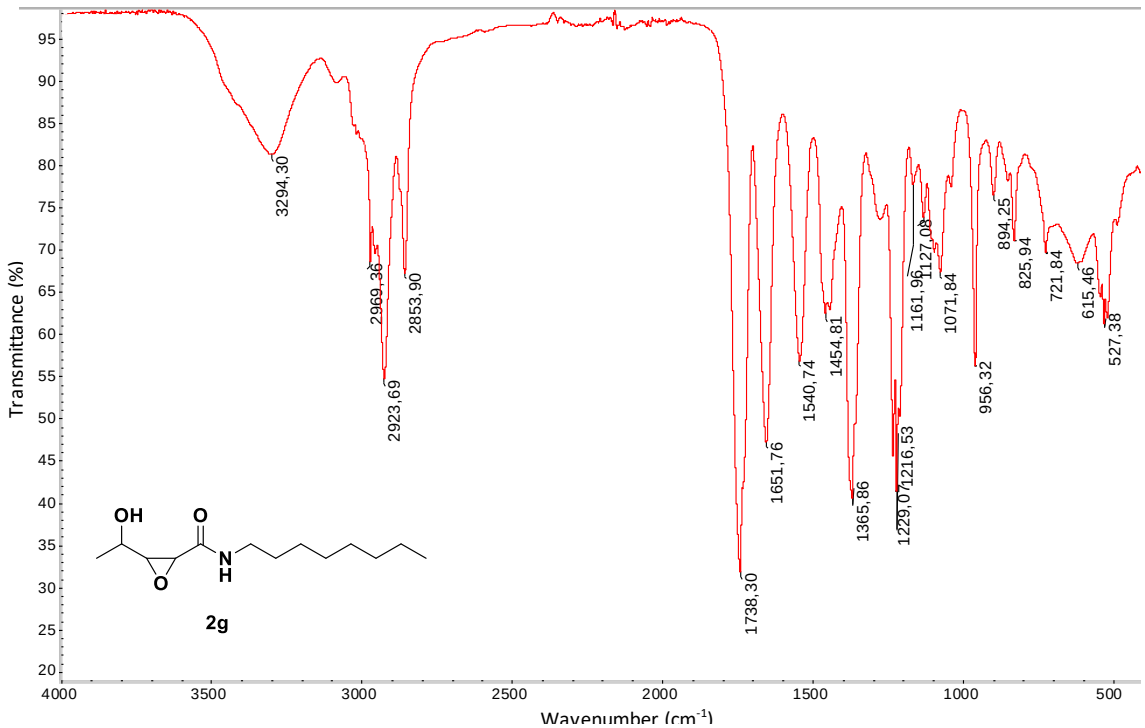
Transmittance (%)
Wavenumber (cm-1)
3294,30
2969,36
2923,69
2853,90
1738,30
1651,76
1540,74
1454,81
1365,86
1229,01
1216,53
1161,96
1127,08
1071,84
956,32
894,25
825,94
721,84
615,46
527,38
OH
O
N
H
O
2g

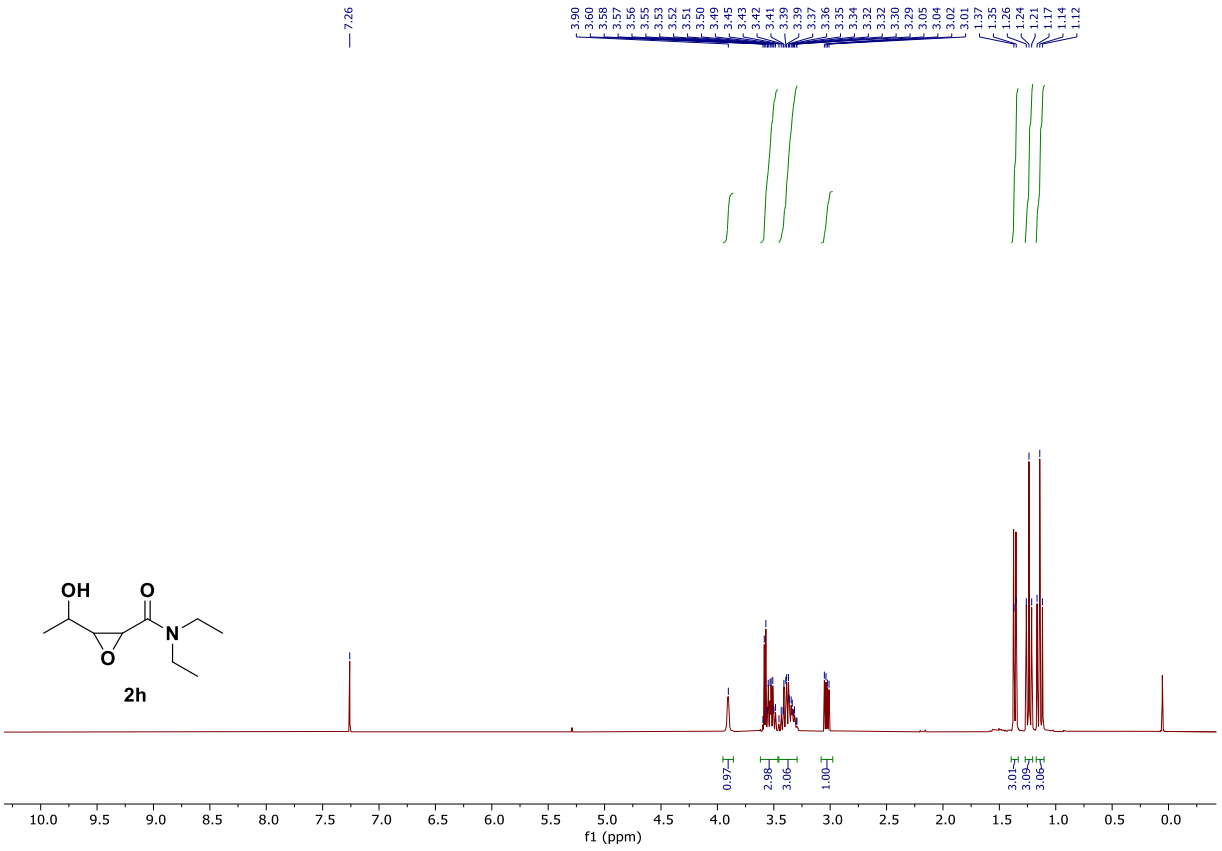
7.26
OH
O
N
O
2h
0.97
2.98
3.06
1.00
3.01
3.09
3.06
f1 (ppm)

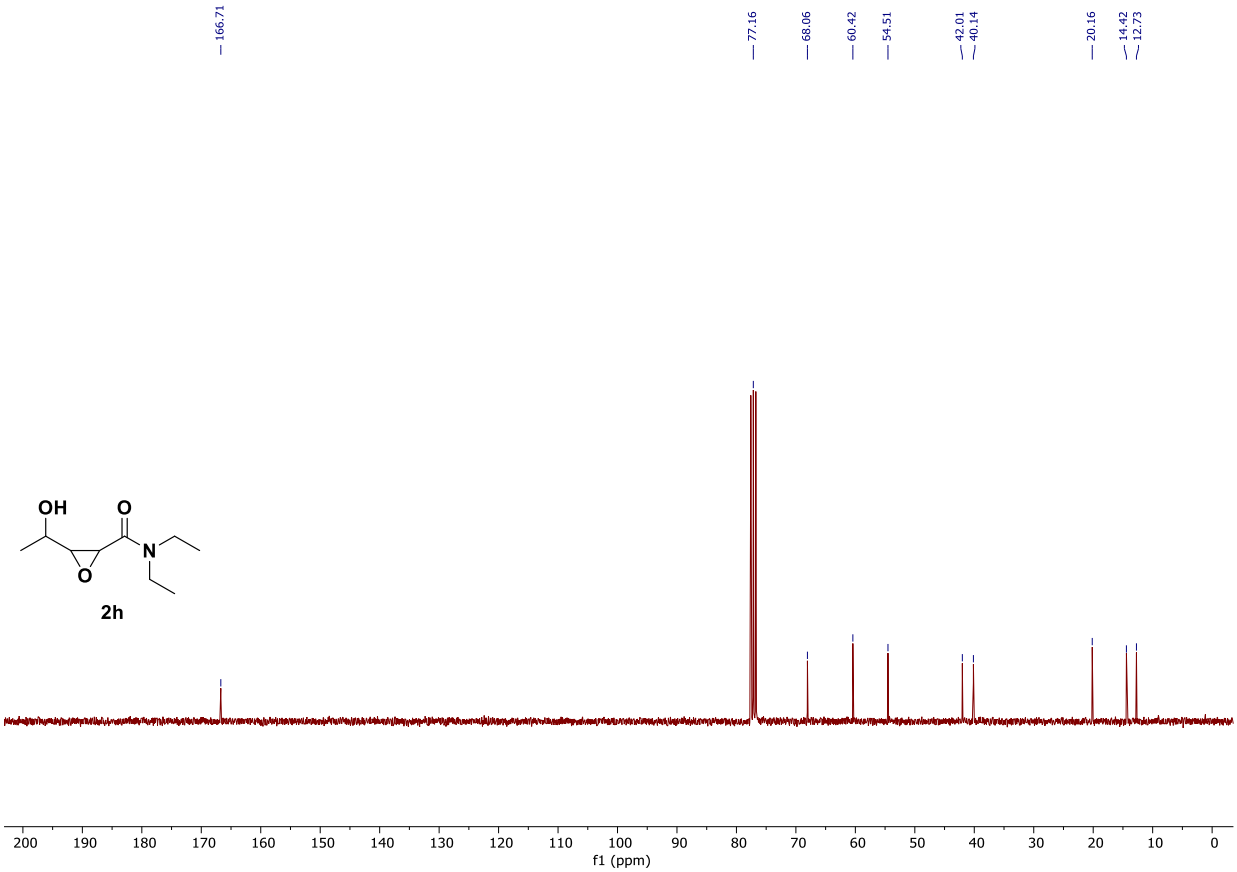
166.71
77.16
68.06
60.42
54.51
42.01
40.14
20.16
14.42
12.73
OH
O
N
O
2h
200 190 180 170 160 150 140 130 120 110 100 90 80 70 60 50 40 30 20 10 0
f1 (ppm)

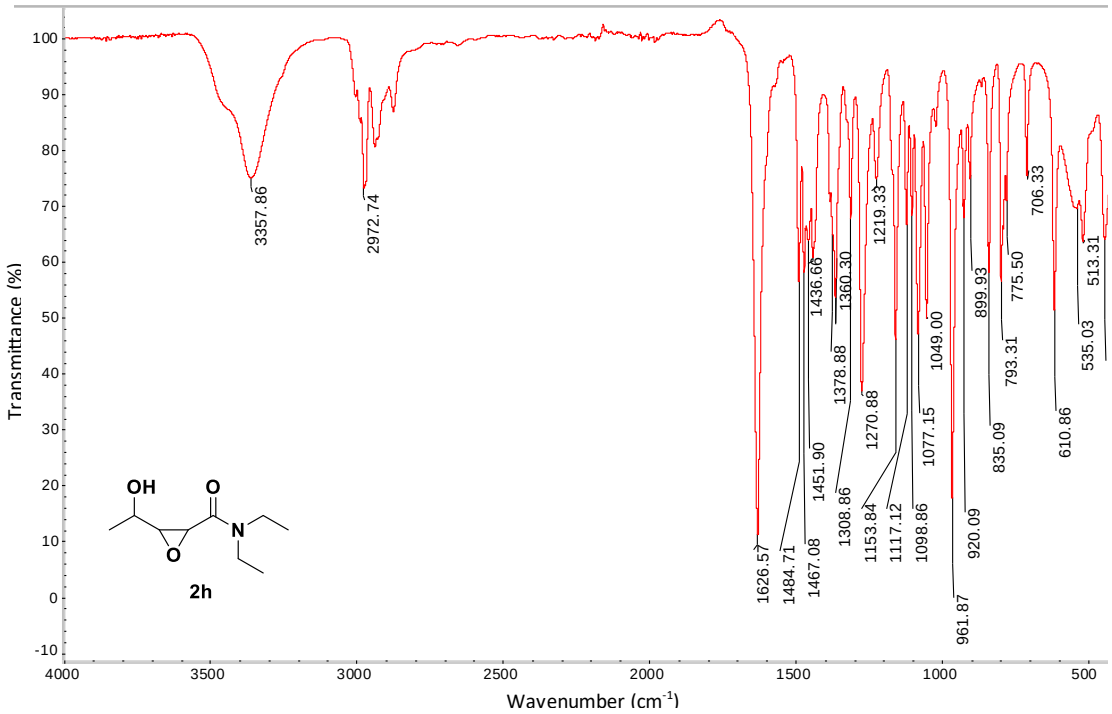
Transmittance (%)
100 90 80 70 60 50 40 30 20 10 0 -10
4000 3500 3000 2500 2000 1500 1000 500
Wavenumber (cm-1)
3357.86
2972.74
1626.57
1484.71
1467.08
1451.90
1436.66
1378.88
1360.30
1308.86
1270.88
1219.33
1153.84
1117.12
1098.86
1077.15
1049.00
961.87
920.09
899.93
835.09
793.31
775.50
706.33
610.86
535.03
513.31
OH
O
N
O
2h

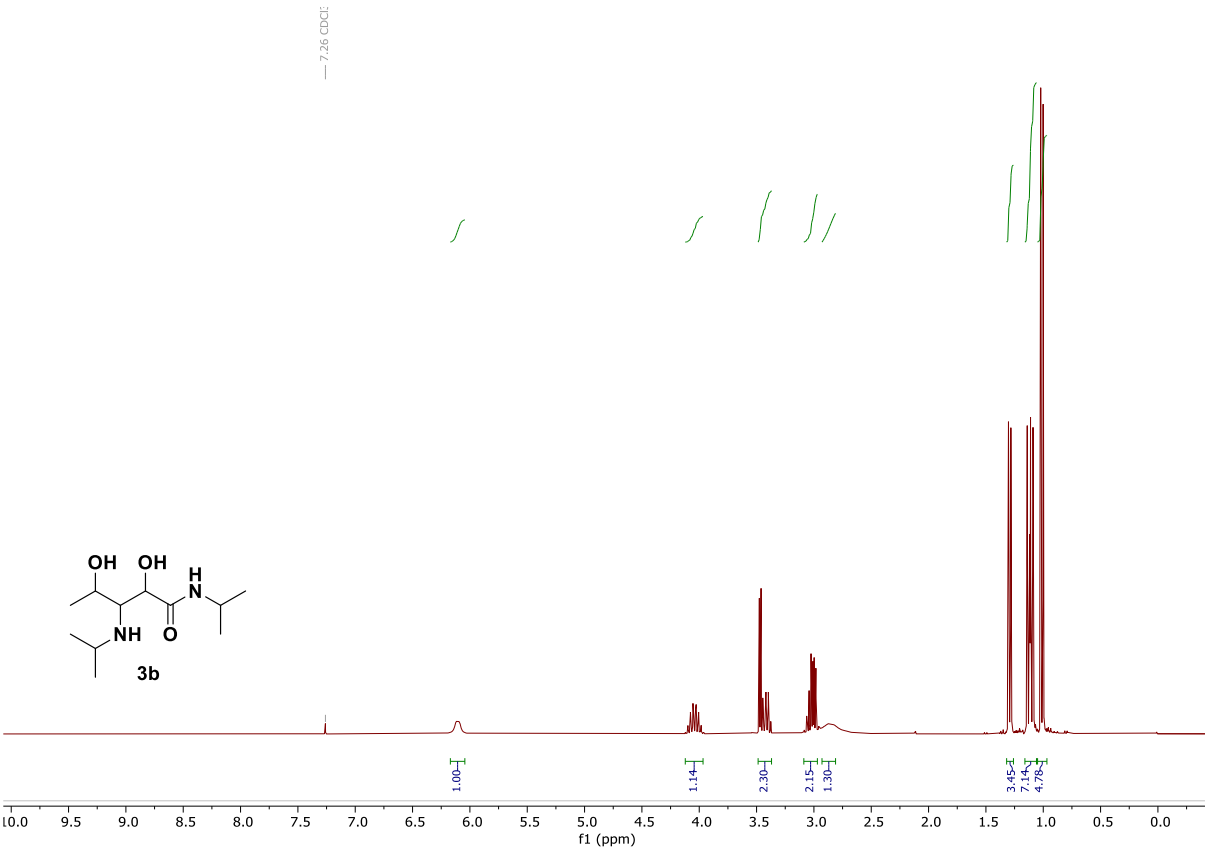
7.26 CDCl3
OH
OH
H
N
NH
O
3b
1.00
1.14
2.30
2.15
1.30
3.45
7.14
4.78
10.0 9.5 9.0 8.5 8.0 7.5 7.0 6.5 6.0 5.5 5.0 4.5 4.0 3.5 3.0 2.5 2.0 1.5 1.0 0.5 0.0
f1 (ppm)

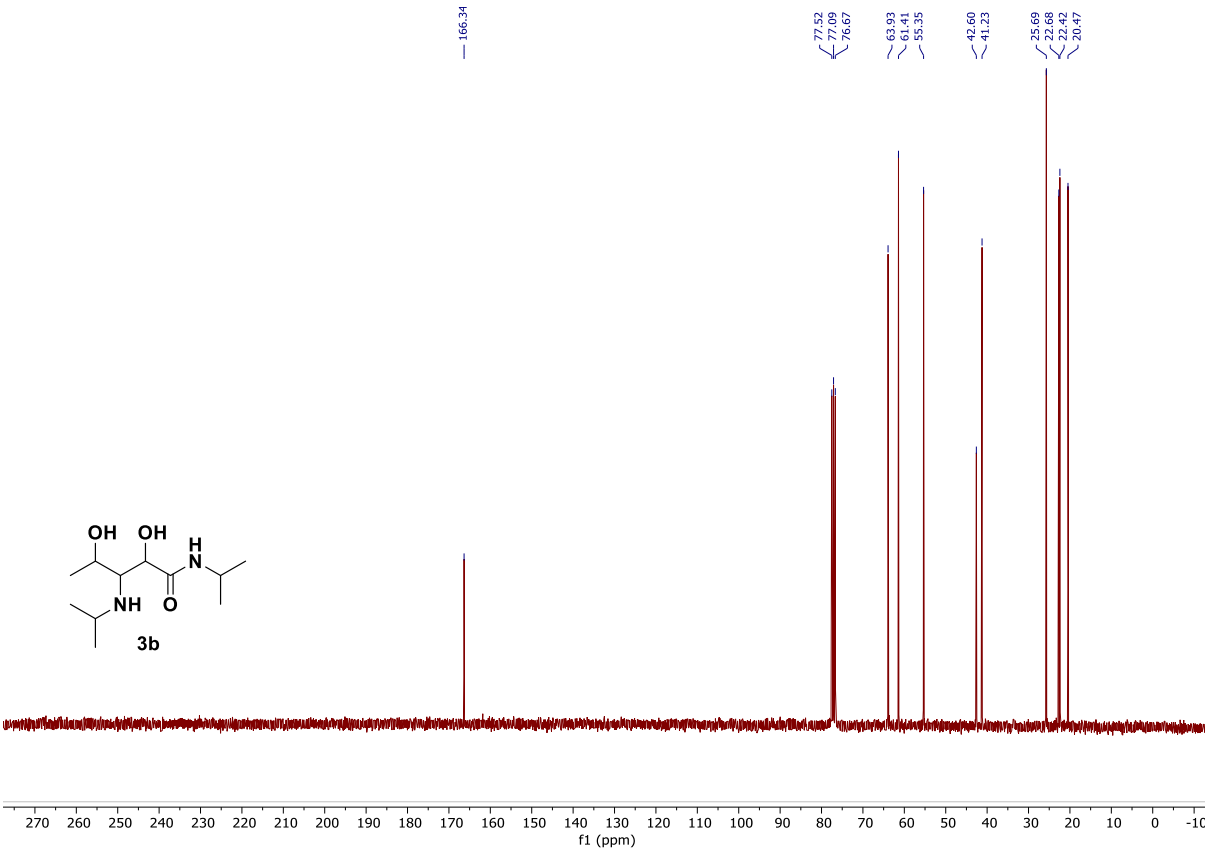
166.34
77.52
77.09
76.67
63.93
61.41
55.35
42.60
41.23
25.69
22.68
22.42
20.47
OH
OH
H
N
NH
O
3b
270 260 250 240 230 220 210 200 190 180 170 160 150 140 130 120 110 100 90 80 70 60 50 40 30 20 10 0 -10
f1 (ppm)

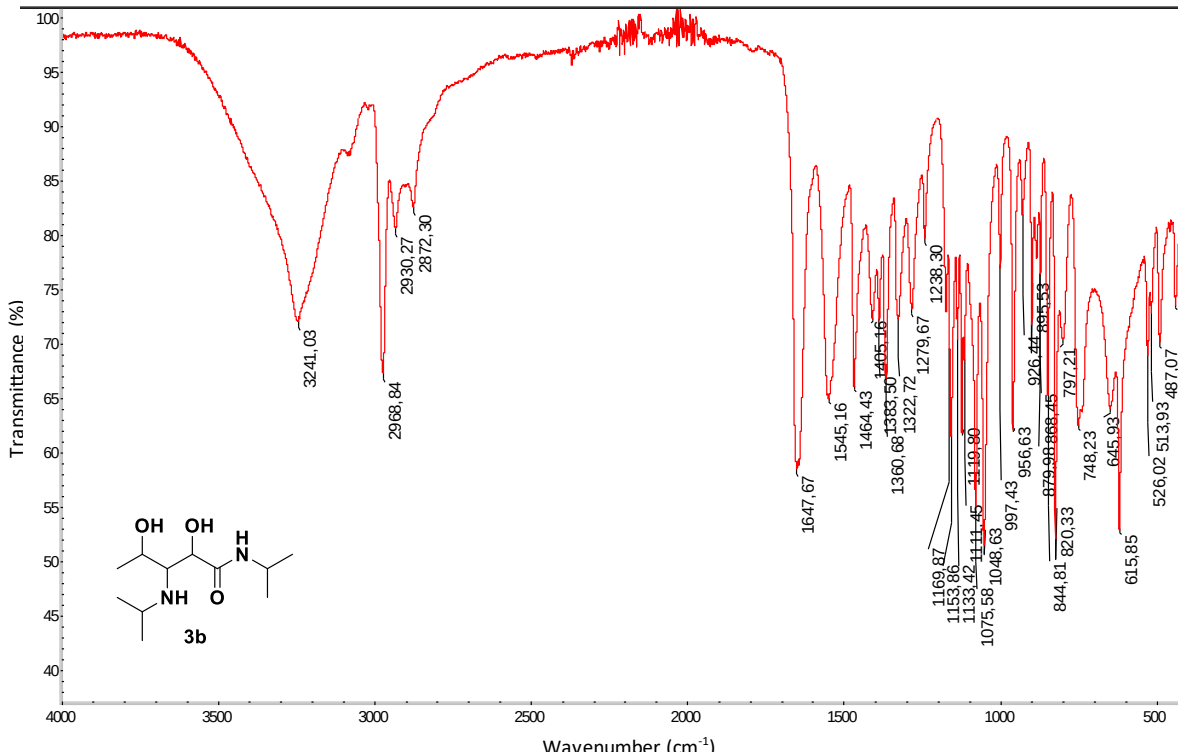
Transmittance (%)
Wavenumber (cm-1)
3241,03
2968,84
2930,27
2872,30
1647,67
1545,16
1464,43
1360,68
1322,72
1279,67
1238,30
997,43
956,63
748,23
645,93
615,85
526,02
513,93
487,07
OH
OH
H
N
NH
O
3b

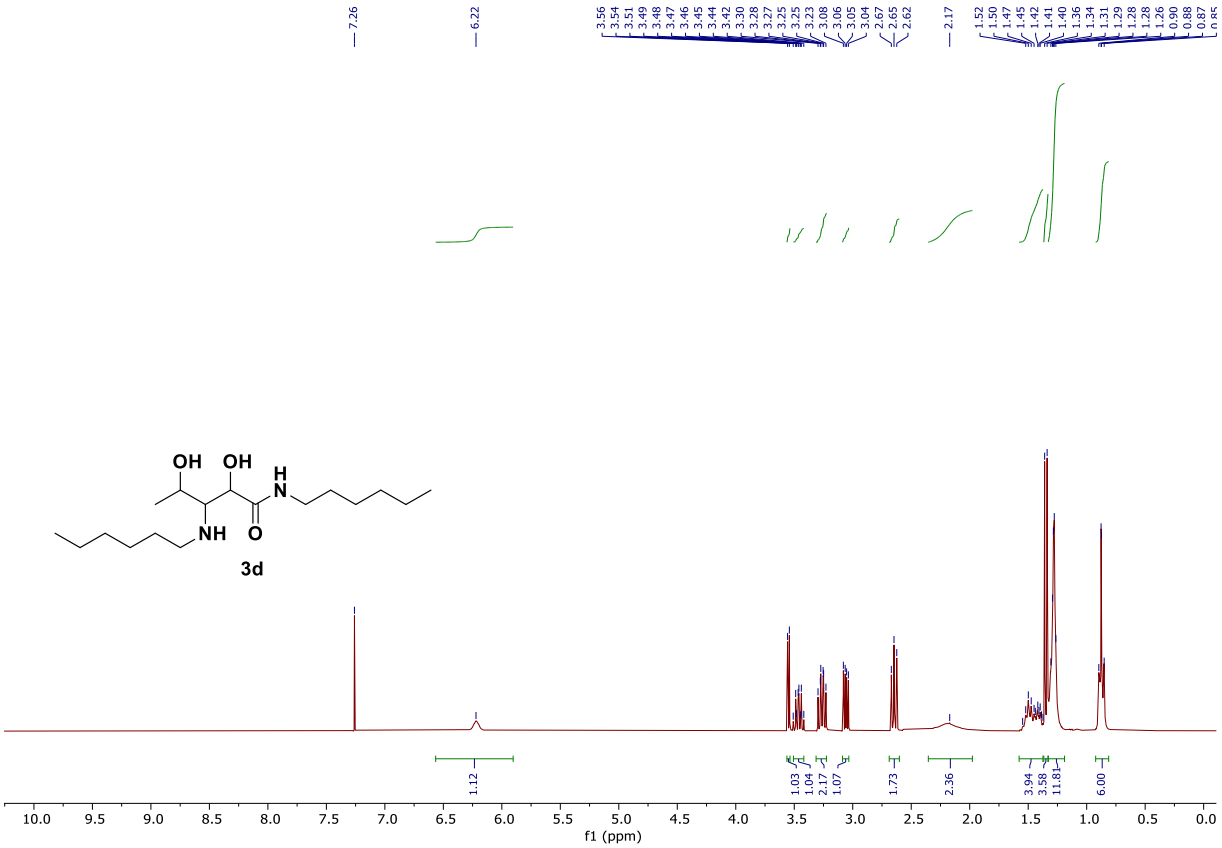
OH
OH
H
N
NH
O
3d
f1 (ppm)

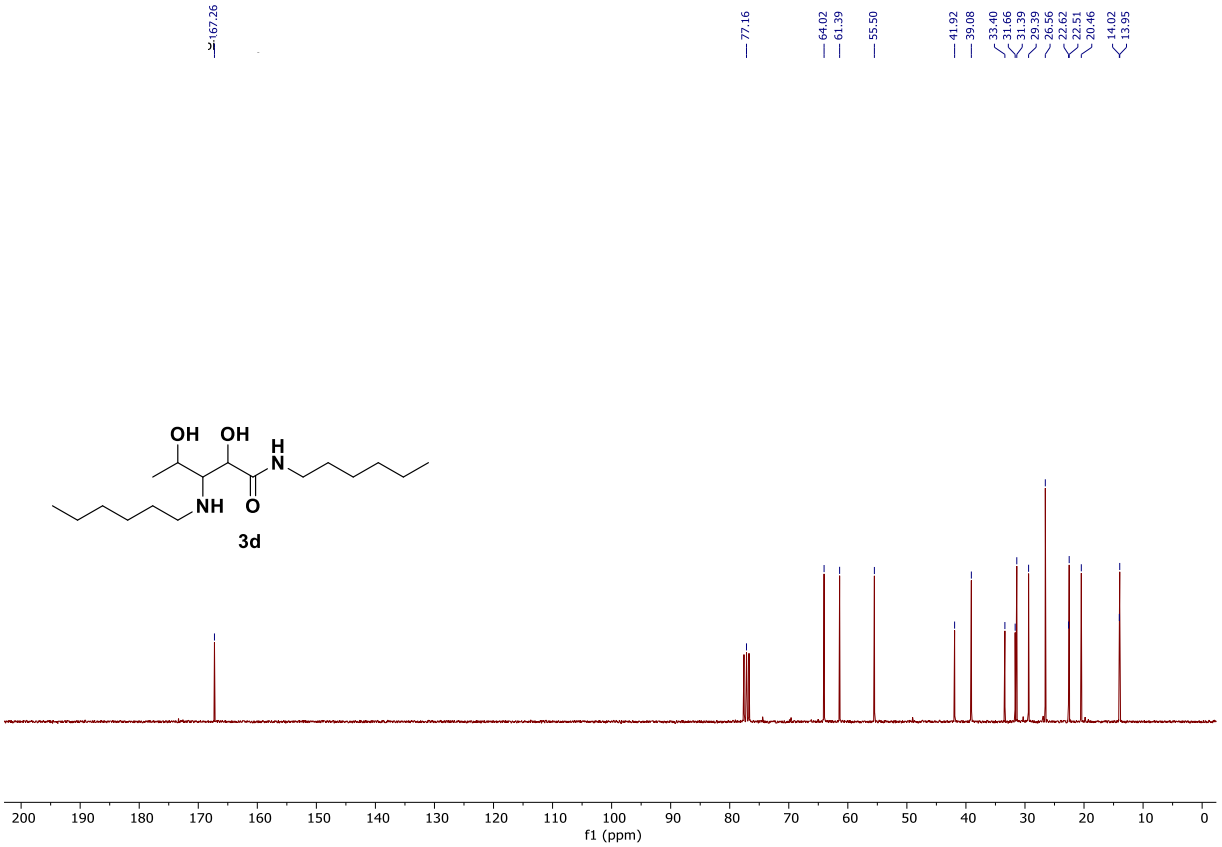
167.26
77.16
64.02
61.39
55.50
41.92
39.08
33.40
31.66
31.39
29.39
26.56
22.62
22.51
20.46
14.02
13.95
OH
OH
H
N
NH
O
3d
200
190
180
170
160
150
140
130
120
110
100
90
80
70
60
50
40
30
20
10
0
f1 (ppm)

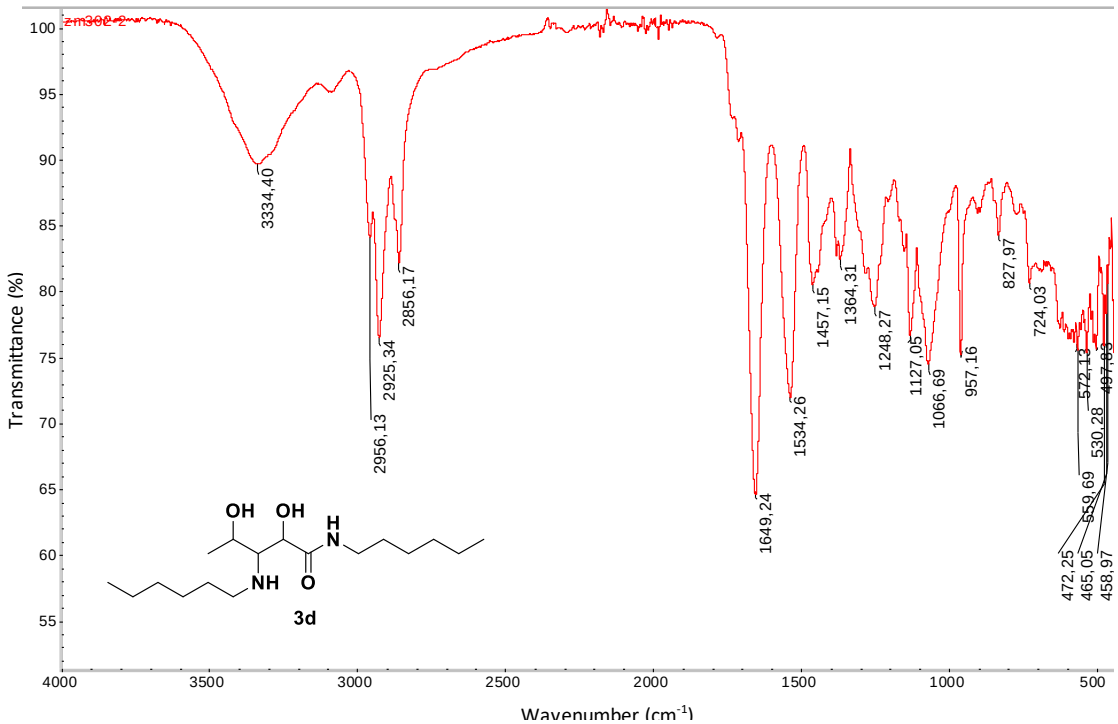
zm302-2
Transmittance (%)
100
95
90
85
80
75
70
65
60
55
3334,40
2956,13
2925,34
2856,17
1649,24
1534,26
1457,15
1364,31
1248,27
1127,05
1066,69
957,16
827,97
724,03
572,13
530,28
497,69
472,25
465,05
458,97
OH
OH
H
N
NH
O
3d
4000
3500
3000
2500
2000
1500
1000
500
Wavenumber (cm-1)

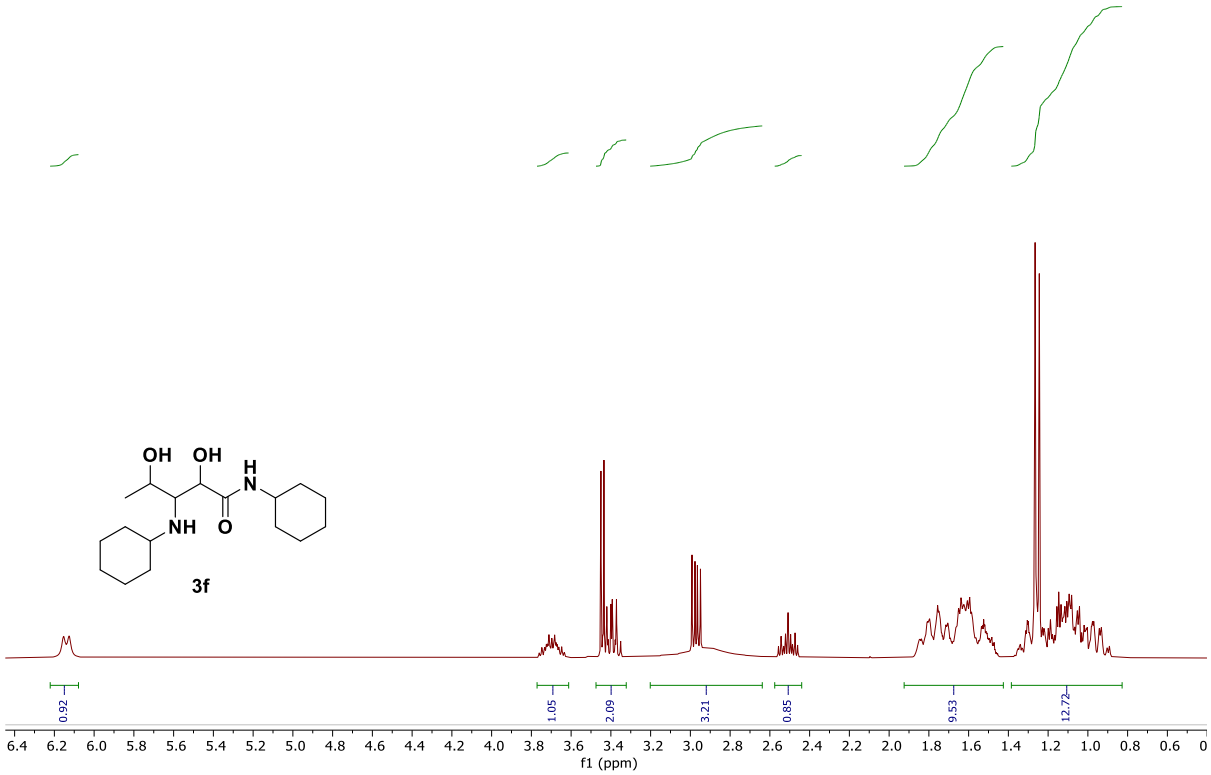
OH
OH
H
N
NH
O
3f
0.92
1.05
2.09
3.21
0.85
9.53
12.72
6.4 6.2 6.0 5.8 5.6 5.4 5.2 5.0 4.8 4.6 4.4 4.2 4.0 3.8 3.6 3.4 3.2 3.0 2.8 2.6 2.4 2.2 2.0 1.8 1.6 1.4 1.2 1.0 0.8 0.6 0
f1 (ppm)

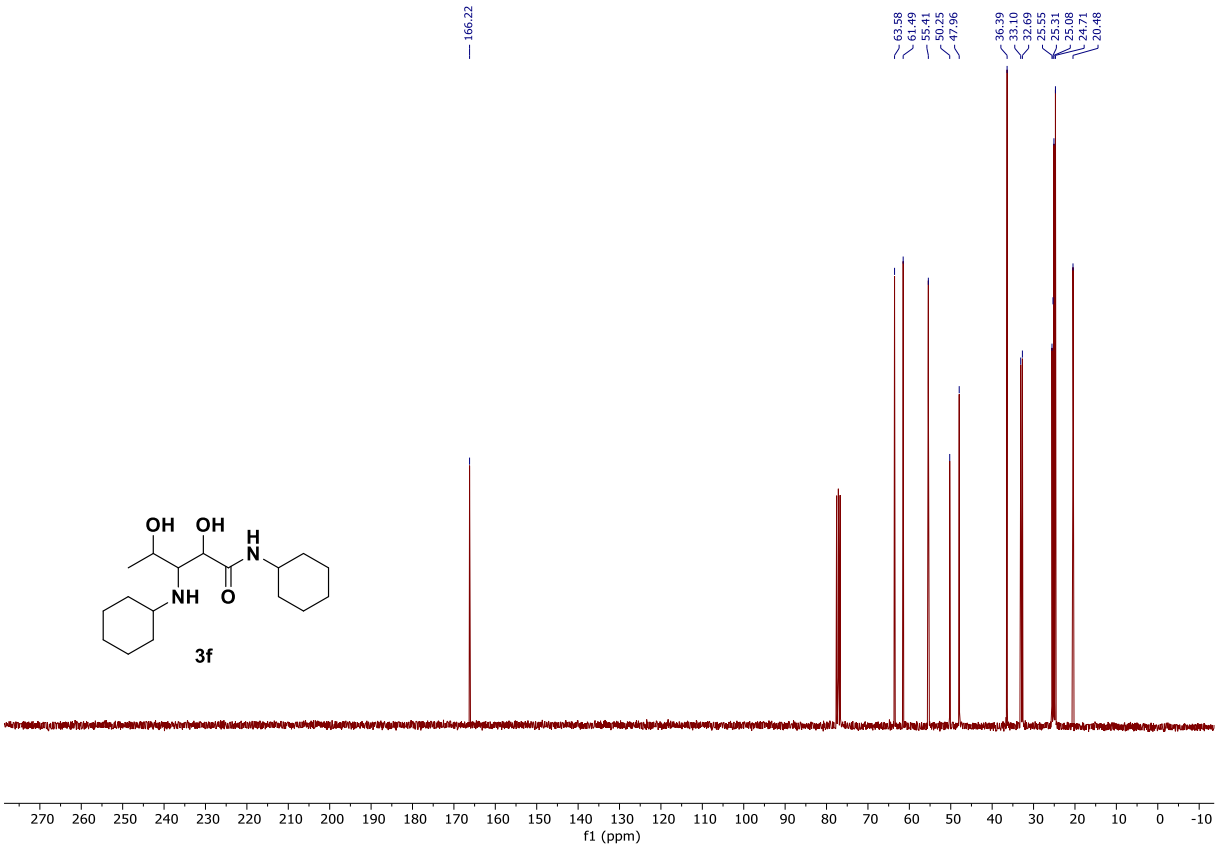
166.22
63.58
61.49
55.41
50.25
47.96
36.39
33.10
32.69
25.55
25.31
25.08
24.71
20.48
OH
OH
H
N
NH
O
3f
270 260 250 240 230 220 210 200 190 180 170 160 150 140 130 120 110 100 90 80 70 60 50 40 30 20 10 0 -10
f1 (ppm)

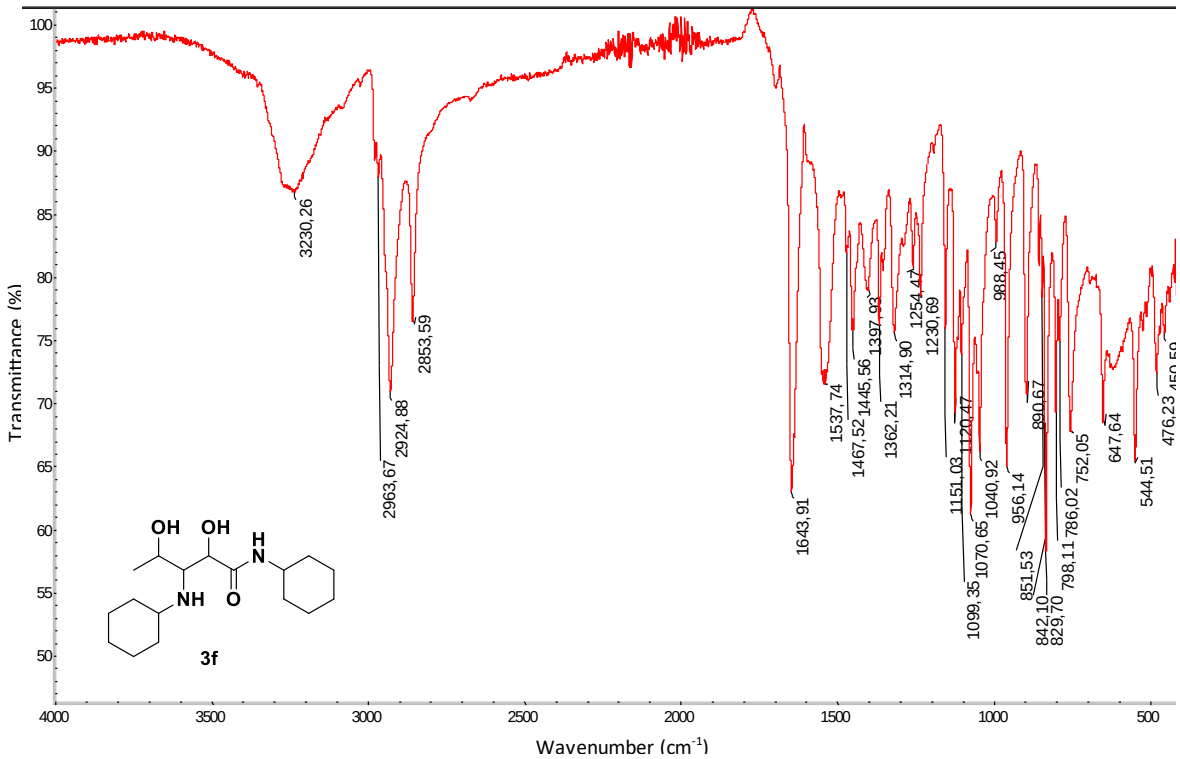
Transmittance (%)
Wavenumber (cm-1)
3230,26
2963,67
2924,88
2853,59
1643,91
1537,74
1467,52
1445,56
1397,93
1362,21
1314,90
1254,47
1230,69
1151,03
1120,47
1099,35
1070,65
1040,92
988,45
956,14
890,67
851,53
842,10
829,70
798,11
786,02
752,05
647,64
544,51
476,23
OH OH
H
N
NH O
3f

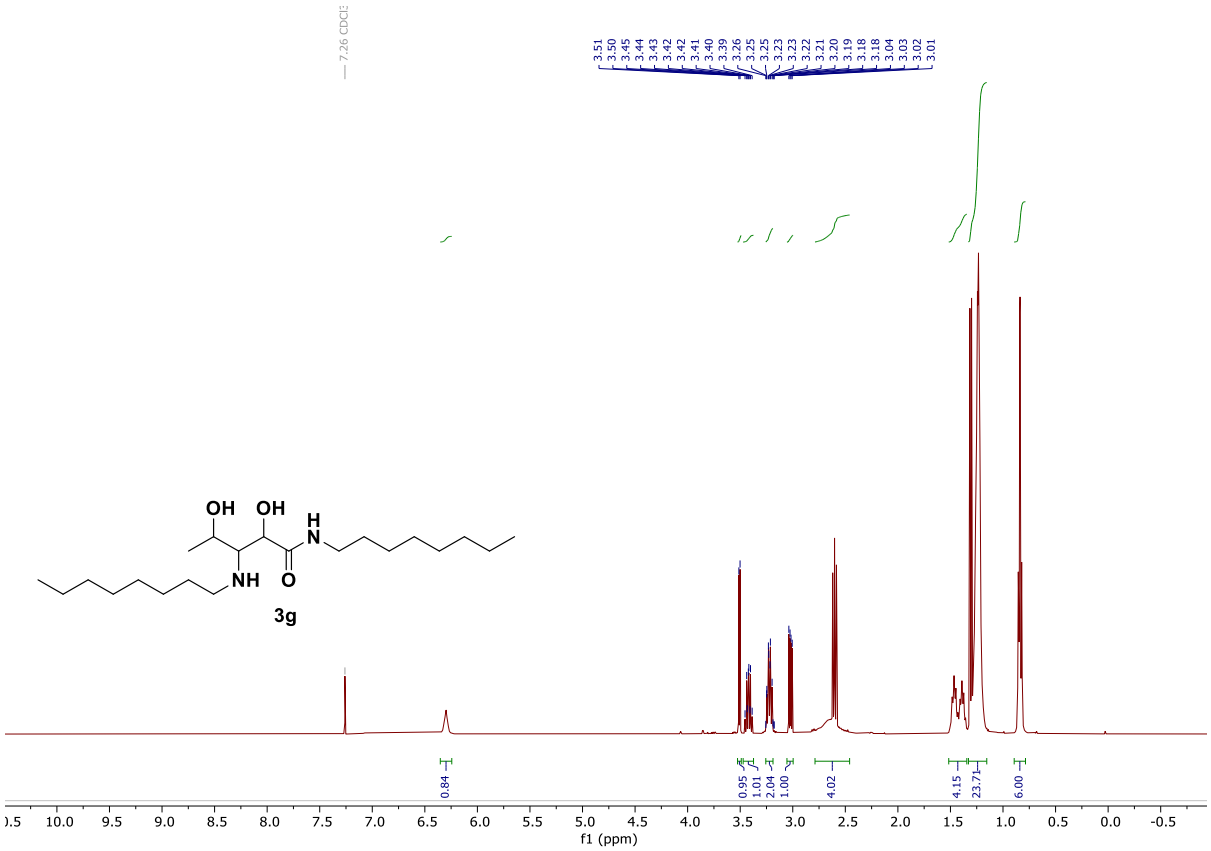
7.26 CDCl3
3.51
3.50
3.45
3.44
3.43
3.42
3.42
3.41
3.40
3.39
3.26
3.25
3.25
3.23
3.23
3.22
3.21
3.20
3.19
3.18
3.18
3.04
3.03
3.02
3.01
OH OH
H
N
NH O
3g
0.84
0.95
1.01
2.04
1.00
4.02
4.15
23.71
6.00
f1 (ppm)

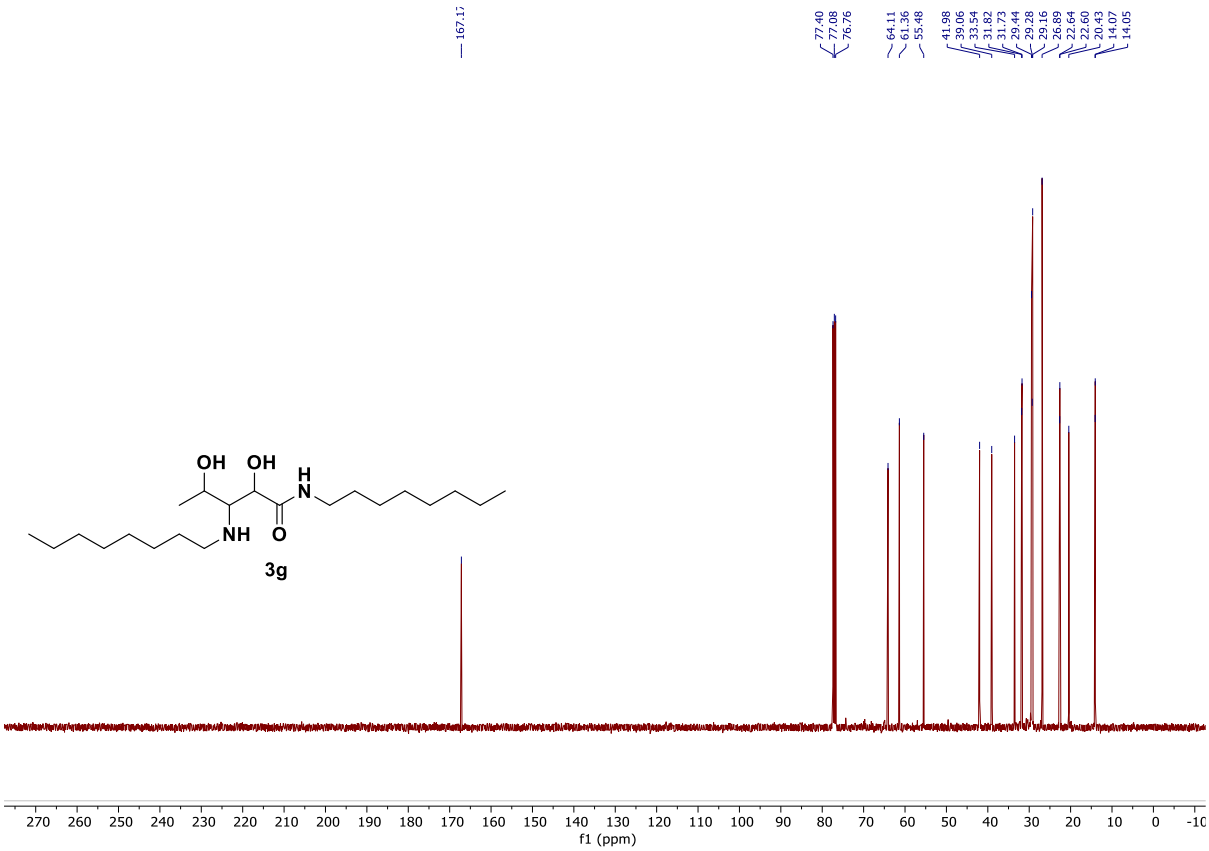
167.17
77.40
77.08
76.76
64.11
61.36
55.48
41.98
39.06
33.54
31.82
31.73
29.44
29.28
29.16
26.89
22.64
22.60
20.43
14.07
14.05
OH
OH
H
N
NH
O
3g
f1 (ppm)

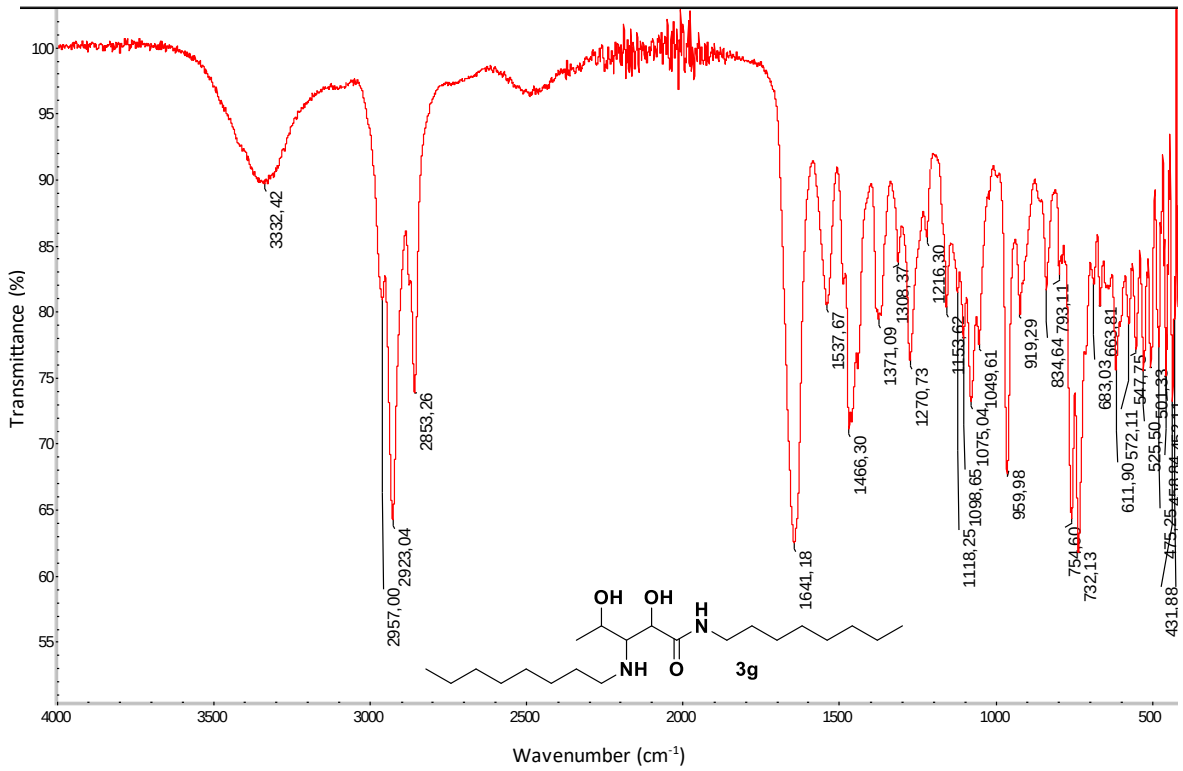
Transmittance (%)
3332,42
2957,00
2923,04
2853,26
1641,18
1537,67
1466,30
1371,09
1308,37
1270,73
1216,30
1153,62
1118,25
1098,65
1075,04
1049,61
959,98
919,29
834,64
793,11
754,60
732,13
683,03
663,81
611,90
572,11
547,75
525,50
501,33
431,88
OH
OH
H
N
NH
O
3g
Wavenumber (cm-1)

References

1 A. Dell'Acqua, B. M. Stadler, S. Kirchhecker, S. Tin, J. G. de Vries, *Green Chem.* 2020, **22**, 5267-5273.

2 R. M. Ortuño, J. Cardellach, J. Font, *J. Heterocyclic Chem.* 1987, **24**, 79.

3 *Gaussian 16, Revision C.01,* M. J. Frisch, G. W. Trucks, H. B. Schlegel, G. E. Scuseria, M. A. Robb, J. R. Cheeseman, G. Scalmani, V. Barone, G. A. Petersson, H. Nakatsuji, X. Li, M. Caricato, A. V. Marenich, J. Bloino, B. G. Janesko, R. Gomperts, B. Mennucci, H. P. Hratchian, J. V. Ortiz, A. F. Izmaylov, J. L. Sonnenberg, D. Williams-Young, F. Ding, F. Lipparini, F. Egidi, J. Goings, B. Peng, A. Petrone, T. Henderson, D. Ranasinghe, V. G. Zakrzewski, J. Gao, N. Rega, G. Zheng, W. Liang, M. Hada, M. Ehara, K. Toyota, R. Fukuda, J. Hasegawa, M. Ishida, T. Nakajima, Y. Honda, O. Kitao, H. Nakai, T. Vreven, K. Throssell, J. A. Montgomery, Jr., J. E. Peralta, F. Ogliaro, M. J. Bearpark, J. J. Heyd, E. N. Brothers, K. N. Kudin, V. N. Staroverov, T. A. Keith, R. Kobayashi, J. Normand, K. Raghavachari, A. P. Rendell, J. C. Burant, S. S. Iyengar, J. Tomasi, M. Cossi, J. M. Millam, M. Klene, C. Adamo, R. Cammi, J. W. Ochterski, R. L. Martin, K. Morokuma, O. Farkas, J. B. Foresman, and D. J. Fox, Gaussian, Inc., Wallingford CT, 2016.

4 (a) E. D. Glendening, J. K. Badenhoop, A. E. Reed, J. E. Carpenter, J. A. Bohmann, C. M. Morales, C. R. Landis, F. Weinhold, *NBO 6.0*, Theoretical Chemistry Institute, University of Wisconsin, Madison, 2013; (b) J. E. Carpenter, F. Weinhold, *J. Mol. Struct.: THEOCHEM* 1988, ***169***, 41-62; (c) F. Weinhold, J. E. Carpenter, *The Structure of Small Molecules and Ions*, Plenum Press, 1988; d) F. Weinhold, C. R. Landis, *Valency and Bonding. A Natural Bond Orbital Donor-Acceptor Perspective*, Cambridge University Press, 2005.

5 J. Bresien, SLURM interface for ORCA and Gaussian, University of Rostock, 2020.

6 A. D. Becke, *J. Chem. Phys.* 1993, **98**, 5648.

7 (a) S. Grimme, J. Antony, S. Ehrlich, H. Krieg, *J. Chem. Phys.* 2010, **132**, 154104; (b) S. Grimme, S. Ehrlich, L. Goerigk, *J. Comput. Chem.* 2011, **32**, 1456.

8 (a) F. Weigend, R. Ahlrichs, *Phys. Chem. Chem. Phys.* 2005, **7**, 3297; (b) F. Weigend, *Phys. Chem. Chem. Phys.* 2006, **8**, 1057.

9 T. Lu, F. Chen, *J. Comput. Chem.* 2012, **33**, 580.

10 R. G. Parr, W. Yang, *J. Am. Chem. Soc.* 1984, **106**, 4049.

11 C. Morell, A. Grand, A. Toro-Labbe, *J. Phys. Chem. A* 2005, **109**, 205.

12 G. M. Sheldrick, *Acta Crystallogr. Sect. A* 2008, **64**, 112-122.

13 G. M. Sheldrick, *Acta Crystallogr. Sect. C* 2015, **71**, 3-8.

14 SADABS within APEX2; Bruker AXS Inc.: Madison, WI, **2014**.